Geochemistry, Geophysics, Geosystems

RESEARCH ARTICLE
10.1029/2018GC008153

Special Section:
Carbon degassing through volcanoes and active tectonic regions

Noble Gas and Carbon Isotope Systematics at the Seemingly Inactive Ciomadul Volcano (Eastern-Central Europe, Romania): Evidence for Volcanic Degassing

B. M. Kis[1,2,3], A. Caracausi[4], L. Palcsu[3], C. Baciu[5], A. Ionescu[1,5,6], I. Futó[3], A. Sciarra[7], and Sz. Harangi[1,8]

[1]MTA-ELTE Volcanology Research Group, Budapest, Hungary, [2]Faculty of Biology and Geology, Babes-Bolyai University, Cluj-Napoca, Romania, [3]Isotope Climatology and Environmental Research Centre, Institute for Nuclear Research, Hungarian Academy of Sciences, Debrecen, Hungary, [4]Istituto Nazionale di Geofisica e Vulcanologia, Palermo, Italy, [5]Faculty of Environmental Science and Engineering, Babes-Bolyai University, Cluj-Napoca, Romania, [6]Department of Physics and Geology, University of Perugia, Perugia, Italy, [7]Istituto Nazionale di Geofisica e Vulcanologia, Rome, Italy, [8]Department of Petrology and Geochemistry, Eötvös Loránd University, Budapest, Hungary

Key Points:
- CO_2 emissions at Ciomadul, Eastern-Central Europe, suggest a still-active plumbing system beneath the volcano in spite of long dormancy
- The CO_2 and He isotope compositions provide evidence for significant contribution of magma-derived volatiles, up to 80%
- Isotopic signatures of gases indicate that primary magmas could have derived from a mantle source modified by subduction-related fluids

Correspondence to:
B. M. Kis,
kis.boglarka@ubbcluj.ro

Citation:
Kis, B. M., Caracausi, A., Palcsu, L., Baciu, C., Ionescu, A., Futó, I., et al. (2019). Noble gas and carbon isotope systematics at the seemingly inactive Ciomadul volcano (Eastern-Central Europe, Romania): Evidence for volcanic degassing. *Geochemistry, Geophysics, Geosystems*, *20*, 3019–3043. https://doi.org/10.1029/2018GC008153

Received 17 DEC 2018
Accepted 5 MAY 2019
Accepted article online 17 MAY 2019
Published online 25 JUN 2019

Abstract Ciomadul is the youngest volcano in the Carpathian-Pannonian Region, Eastern-Central Europe, which last erupted 30 ka. This volcano is considered to be inactive, however, combined evidence from petrologic and magnetotelluric data, as well as seismic tomography studies, suggests the existence of a subvolcanic crystal mush with variable melt content. The volcanic area is characterized by high CO_2 gas output rate, with a minimum of 8.7×10^3 t/year. We investigated 31 gas emissions at Ciomadul to constrain the origin of the volatiles. The $\delta^{13}C$–CO_2 and $^3He/^4He$ compositions suggest the outgassing of a significant component of mantle-derived fluids. The He isotope signature in the outgassing fluids (up to 3.10 R_a) is lower than the values in the peridotite xenoliths of the nearby alkaline basalt volcanic field (R/R_a 5.95 $R_a \pm$ 0.01), which are representative of a continental lithospheric mantle and significantly lower than MORB values. Considering the chemical characteristics of the Ciomadul dacite, including trace element and Sr–Nd and O isotope compositions, an upper crustal contamination is less probable, whereas the primary magmas could have been derived from an enriched mantle source. The low He isotopic ratios could indicate a strongly metasomatized mantle lithosphere. This could be due to infiltration of subduction-related fluids and postmetasomatic ingrowth of radiogenic He. The metasomatic fluids are inferred to have contained subducted carbonate material resulting in a heavier carbon isotope composition ($\delta^{13}C$ is in the range of −1.4‰ to −4.6‰) and an increase of $CO_2/^3He$ ratio. Our study shows the magmatic contribution to the emitted gases.

Plain Language Summary Determining the fluxes and composition of gases in active and dormant volcanoes could help to constrain their origin. Ciomadul is the youngest volcano of the Carpathian-Pannonian Region, Eastern-Central Europe, where the last eruption occurred 30 ka. Its eruption chronology is punctuated by long quiescence periods (even >100 kyr) separating the active phases; therefore, the long dormancy since the last eruption (30 ka) does not unambiguously indicate inactivity. Knowing if melt-bearing magma resides in the crust is fundamental to evaluate the nature of the volcano. Isotopic compositions of helium ($^3He/^4He$) and carbon ($\delta^{13}C_{CO2}$) are important tools for the study of the origin of the gases. We show that the isotope variation of the emitted gases suggests a metasomatized lithospheric mantle origin for the primary magmas. This is consistent with a degassing deep magma body existing beneath Ciomadul, and this long-dormant volcano cannot be considered as extinct.

1. Introduction

Gas emissions are often associated with active or dormant volcanic areas and regions affected by extensional tectonics (e.g., O'Nions & Oxburgh, 1988; Oppenheimer et al., 2014). Monitoring of fluids (chemical and isotopic compositions and physical properties) in volcanic regions provides important information concerning the processes occurring at depth (e.g., Agusto et al., 2013; Barry et al., 2013, 2014; Caliro et al., 2015; Christopher et al., 2010; Edmonds, 2008; Fischer, 2008; Mazot et al., 2011; Roulleau et al., 2016; Ruzié et al., 2012; Tassi et al., 2010, 2011, 2016; Wei et al., 2016). The chemical and isotopic composition of the

emitted fluids in active volcanoes is primarily controlled by magmatic processes, such as the injection of new magma into the plumbing system or degassing of deep mafic magma in the lower crust, or interaction with the volcanic hydrothermal systems, among others (e.g., Caracausi et al., 2003, 2013; Christopher et al., 2010; Edmonds, 2008; Paonita et al., 2012, 2016; Sano et al., 2015). Furthermore, compositional change of the fluids may also correlate with the seismicity at regional scale (e.g., Bräuer et al., 2008, 2018; Cardellini et al., 2017; Chiodini et al., 2004; Melián et al., 2012).

There has been major progress in understanding the factors controlling gas emissions in active and dormant volcanic areas during the last two decades (Aiuppa et al., 2007; Edmonds, 2008; Lee et al., 2016; Moussallam et al., 2018; Oppenheimer et al., 2014); however, much less attention has been given to seemingly inactive volcanic areas (Roulleau et al., 2015). These are volcanoes that last erupted more than 10 ka, and at the surface, there are no signs of reawakening. The Tatun volcanic complex in Taiwan is an example of such a volcanic system. Although the last eruption occurred 20 ka, geophysical data indicate a still-active magma storage. The composition of emitted gases is consistent with this interpretation, as they contain significant magmatic components (Roulleau et al., 2015). The importance and the potential hazard of such volcanoes are shown by the case of the Ontake volcano in Japan. There were no proven records of historical and even Holocene eruptions before the phreatic eruptive event in 1979, and therefore, there were no detailed studies and monitoring on this volcano. In 2014, another phreatic eruption occurred, causing serious fatalities (Kato et al., 2015) and pointed to the requirement to better understand such long-dormant volcanoes. Sano et al., 2015 demonstrated that regular monitoring of volcanic gases is fundamental to understand the behavior of these apparently inactive volcanoes. In this regard, detection of a magmatic chamber containing some melt fraction could mean the potential for reactivation even after several tens of kiloyears dormancy. Emission of gases with isotopic signatures in the range of magmatic values can be evidence of magma intrusions at depth (Bräuer et al., 2008, 2018; Caracausi et al., 2013, 2015; Carapezza et al., 2003, 2012; Carapezza & Tarchini, 2007; Farrar et al., 1995; Fischer et al., 2014; Pizzino et al., 2002; Rouwet et al., 2014, 2017; Sano et al., 2015; Sorey et al., 1998), in addition to recognition of geophysical anomalies reflecting melt pockets at depth (Comeau et al., 2015, 2016; Harangi, Novák, et al., 2015).

Ciomadul is the youngest volcano within the Carpathian-Pannonian Region, Eastern-Central Europe, where the last eruption occurred 30 ka (Harangi et al., 2010; Harangi, Lukács, et al., 2015; Molnár et al., 2019). Thus, it is usually considered as an inactive volcano. In spite of its long dormancy, combined evidence from petrologic and magnetotelluric data (Harangi, Novák, et al., 2015; Kiss et al., 2014), as well as seismic tomography (Popa et al., 2012), suggest the presence of a melt-bearing crystal mush beneath the volcano. This is consistent with the local high heat flow (85–120 mW/m^2) compared to the Carpathian Range where this value decreases to 40–60 mW/m^2 (Demetrescu & Andreescu, 1994; Horváth et al., 2006), the high flux of carbon dioxide of 8.7×10^3 t/year (Kis et al., 2017) the presence of mineral and thermal waters up to 78 °C (Jánosi, 1980; Rădulescu et al., 1981) and the geodynamically active region (Ismail-Zadeh et al., 2012; Wenzel et al., 1999). The eruption chronology of the Ciomadul lava dome field (Molnár et al., 2018) is characterized by prolonged quiescence periods between the active phases, often exceeding 100 kyr.

There are a number of sites at Ciomadul, where significant amount of CO_2 gases are emitted (Kis et al., 2017). Althaus et al. (2000), Vaselli et al. (2002), Frunzeti (2013), and Sarbu et al. (2018) studied the composition of gases collected from a few locations and concluded that they could indicate a deep-seated magma body below the volcano. Here we present a comprehensive helium isotope signature (hereafter $^3He/^4He$) and carbon isotope (hereafter $\delta^{13}C_{CO2}$) systematics of the volatile degassing from Ciomadul based on a detailed sampling of all the main known locations of gas emissions to constrain the origin of fluids and to characterize the nature of a seemingly inactive volcano.

2. Geological Setting

2.1. Ciomadul Volcanic Dome Field

Ciomadul volcano is located at the southeastern edge of the Carpathian-Pannonian Region, at the southern end of the Călimani-Gurghiu-Harghita volcanic chain (Szakács et al., 1993; Szakács & Seghedi, 1995; Pécskay et al., 2006; Figure 1). It is part of a postcollisional volcanic belt, which comprises a series of andesitic to dacitic volcanoes, developed parallel with the Carpathian orogeny. The volcanism occurred well after the continent-continent collision between the Tisza-Dacia microplate and the western margin of the

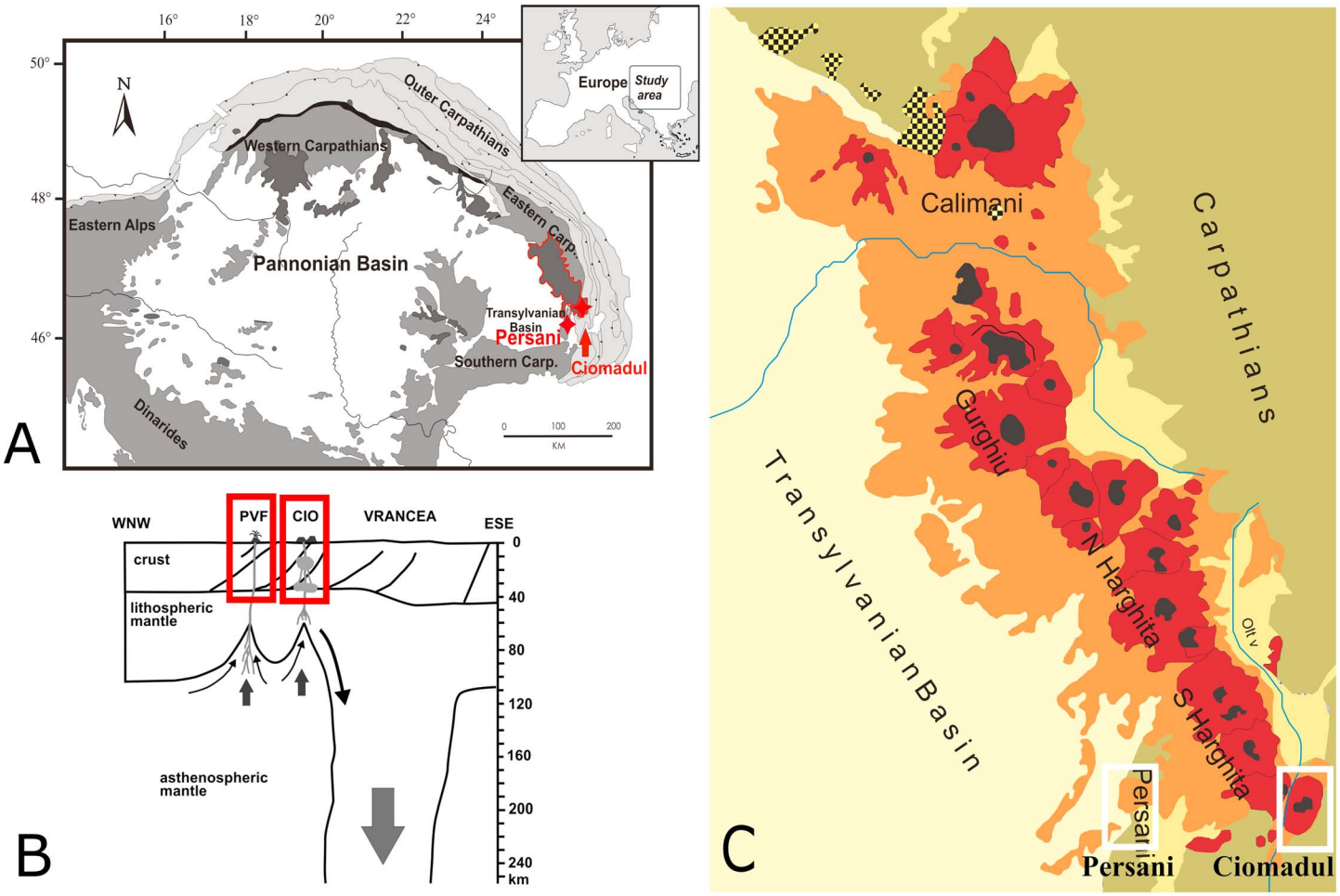

Figure 1. (a) Location of Ciomadul and Persani volcanoes in the southeastern Carpathian area of the Carpathian-Pannonian Region (after Harangi et al., 2013). (b) Geotectonic model of the Persani and Ciomadul volcanic areas. PVF = Persani Volcanic Field; CIO = Ciomadul (after Harangi et al., 2013). (c) Location of Ciomadul and Persani volcanoes in the volcanic range of the Eastern Carpathians (modified after Szakács & Seghedi, 1995).

Eurasian plate (Cloetingh et al., 2004; Csontos et al., 1992; Mațenco et al., 2007; Mațenco & Bertotti, 2000; Seghedi et al., 2004, 2005, 2011). Ciomadul is part of a lava dome field and this central volcanic complex involves 8–14 km^3 of high-K dacitic lavas (Karátson & Timár, 2005; Molnár et al., 2019; Szakács et al., 2015). The volcano developed on the Early Cretaceous clastic flysch sedimentary unit of the Eastern Carpathians that forms several nappes. It consists of binary alternation of sandstones, calcareous sandstones, limestones, and clays/marls from the Sinaia Formation of the Ceahlau nappe and the Bodoc flysch (Băncilă, 1958; Grasu et al., 1996; Ianovici & Rădulescu, 1968; Nicolaescu, 1973). The flysch unit has a thickness up to 2,500 m.

The Ciomadul volcanic complex is made up by amalgamation of several lava domes truncated by two explosion craters called Mohos and Saint Anna (Szakács et al., 2015). This central volcano is surrounded by further isolated lava domes (Baba Laposa, Haramul Mic, Dealul Mare, Büdös-Puturosul and Bálványos; Molnár et al., 2018, Figure 2). Volcanism at the Ciomadul volcanic dome field started around 1 Ma, while the most voluminous Ciomadul volcanic structure has developed over the last approximately 160 kyr (Molnár et al., 2018, 2019). During the first volcanic stage, the intermittent lava dome extrusions were separated by relatively long dormant periods even exceeding 100 kyr. The second volcanic stage was characterized by initial lava dome effusion and then, after approximately 40 kyr of quiescence, a more explosive volcanic activity occurred (from 57 to 30 ka, Harangi et al., 2010; Harangi, Lukács, et al., 2015; Karátson et al., 2016; Molnár et al., 2018, 2019; Moriya et al., 1995, 1996; Vinkler et al., 2007). This stage involved lava-dome collapse events, vulcanian and subplinian to plinian explosive eruptions (Harangi, Lukács,

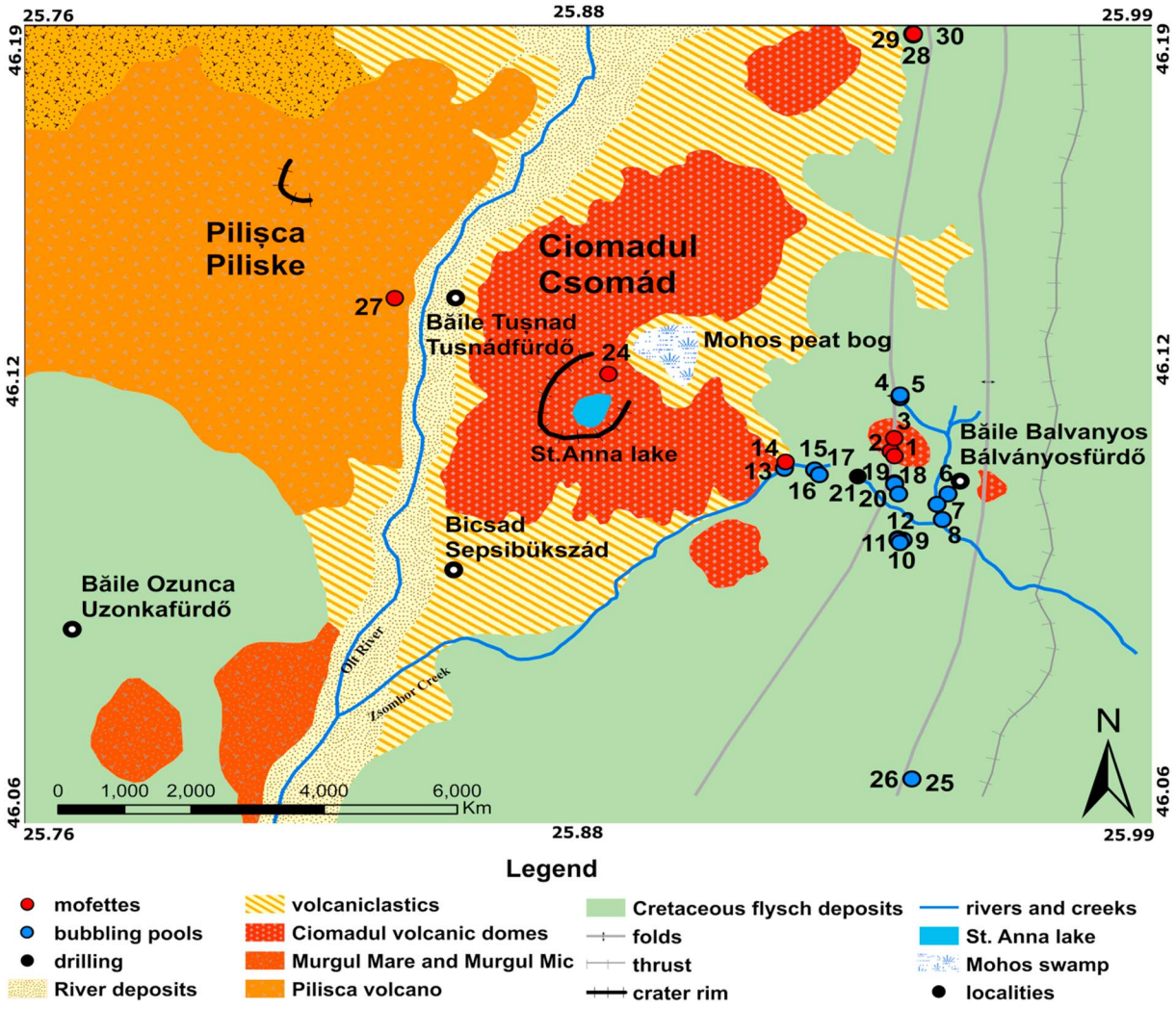

Figure 2. Geological sketch map of the study area. The red, black, and blue dots indicate the type of the sampling points: mofette, drilling, and bubbling pool, respectively. The numbers on the sampling sites are the same as in Table 1. (Geological map is modified after Ianovici & Rădulescu, 1968).

et al., 2015; Karátson et al., 2016; Vinkler et al., 2007). The eruptive products are relatively homogeneous K-rich dacites (Molnár et al., 2018, 2019; Szakács et al., 1993; Szakács & Seghedi, 1987; Vinkler et al., 2007). Petrogenetic and thermobarometric studies on amphiboles as well as combined U-Th/He and U/Th zircon dating suggest the presence of a long-lasting (up to 350 kyr) crystal mush body in the crust. This appears to be mostly at relatively low-temperature just above the solidus (700–750 °C) and is periodically partly remobilized by injections of fresh basaltic magmas that could rapidly trigger volcanic eruptions (Harangi, Lukács, et al., 2015; Harangi, Novák, et al., 2015; Kiss et al., 2014).

The Ciomadul volcano is located near (~50 km) the Vrancea seismic region (Ismail-Zadeh et al., 2012; Wenzel et al., 1999) located at the arc bend between the Eastern and the Southern Carpathians. Frequently occurring earthquakes have deep hypocentres (70–170 km) delineating a narrow, vertical region. This is consistent with a high-velocity seismic anomaly interpreted as a cold lithosphere slab descending slowly into the asthenospheric mantle (Wortel & Spakman, 2000). Further crustal and subcrustal earthquakes ($M < 4$) occur occasionally around the Perşani basalt volcanic field and the Ciomadul volcano (Popa et al., 2012). The seismic tomographic model indicates a vertically extended low-velocity anomaly beneath Ciomadul. This can be interpreted as transcrustal magma storage with an upper melt-dominated magma chamber (Popa et al., 2012). The seismic tomographic model is supported by the result of combined petrologic and magnetotelluric studies that demonstrated the existence of a low-resistivity anomaly and the

depth of 5–20 km beneath the volcanic centers of Ciomadul, inferred to be a melt-bearing crystal mush (Harangi, Novák, et al., 2015). In addition, a deeper low-resistivity anomaly was also detected at a depth of 30–40 km, possibly related to a deeper magma accumulation zone at the crust-mantle boundary.

Another Pleistocene monogenetic basalt volcanic field is approximately 40 km from the Ciomadul, at the southeastern part of the Carpathian-Pannonian Region (Figure 1), at the boundary between the Perşani Mountains and the Transylvanian basin (Downes et al., 1995; Harangi et al., 2013; Seghedi et al., 2016; Seghedi & Szakács, 1994). Basaltic volcanism occurred here between 1.14 Ma and 683 ka (Panaiotu et al., 2004, 2013) and formed several volcanic centers accompanied by maars, scoriacones, and lava flows. The erupted basaltic magma carried significant amount of ultramafic xenoliths from the lithospheric mantle (peridotites and amphibole pyroxenites) revealing the nature of the uppermost mantle of this region (Falus et al., 2008; Vaselli et al., 1995).

2.2. Gas Emissions and Mineral Water Springs at Ciomadul Volcanic Area

Gas emanations in the form of bubbling pools and low-temperature (T ~ 8–10 °C) dry mofettes are characteristic of the Ciomadul volcano. CO_2-bubbling peat bogs can be also found, mainly at the northeastern (Buffogó peat bog) and southern parts of the Puturosul Mountains (Zsombor-Valley, Jánosi et al., 2011). The minimum total CO_2 flux was estimated to be 8.7×10^3 t/year (Kis et al., 2017). The aquifers of this area are represented by CO_2-rich sparkling mineral water, with temperature up to 22.5 °C (Berszán et al., 2009; Italiano et al., 2017; Jánosi et al., 2011).

3. Sampling and Analytical Methods

A total of 31sites were selected for this study, including bubbling pools, dry gas emissions (mofettes), and one drilling (Figure 2 and Table 1). We collected fluids during two field campaigns carried out in the spring and autumn of 2016, respectively. In the first field campaign, gas samples were collected for $\delta^{13}C–CO_2$ and $^3He/^4He$ composition in 1-L evacuated Pyrex glass tubes with a vacuum stopcock, while for chemical composition, gas samples were collected in 150-ml glass tubes with two vacuum stopcocks. Chemical compositions were analyzed at the Istituto Nazionale di Geofisica e Vulcanologia, Rome, Italy, whereas chemical and isotopic composition of water, noble gas compositions (He and Ne) and $\delta^{13}C–CO_2$ of gas samples were measured at the Isotope Climatology and Environmental Research Centre (ICER), Institute for Nuclear Research, Hungarian Academy of Sciences, Debrecen, Hungary. During the second field campaign, the samples were collected in glass and steel samplers equipped with two valves. These samples were analyzed for their elemental composition (He, Ne, Ar, H_2, O_2, N_2, CO, CH_4, and CO_2), $\delta^{13}C$ (CO_2), $^3He/^4He$ ratios, and ^{20}Ne abundances at the Istituto Nazionale di Geofisica e Vulcanologia, Palermo, Italy (INGV-Palermo).

We also separated clinopyroxene mineral grains (>3 g in weight) from one of the lherzolite xenoliths collected at the foot of the Gruiu scoria cone, in the Perșani volcanic field. The noble gas composition of the fluid inclusions was analyzed at INGV-Palermo.

3.1. Chemical and Isotopic Composition of Gases

The chemical composition of the samples from the first campaign was analyzed with a Portable Varian CP4900 Micro Gas Chromatograph (GC). This Micro GC is configured for the analysis of He, Ne, H_2, O_2, and N_2 by means of a molecular sieve 5A (20 m unheated) column and CO_2, CH_4, and H_2S by means of a PoraPlot (PPQ 10 m heated) column. The instrument is equipped with a microthermal conductivity detector responding to the difference in thermal conductivity between the carrier gas (argon) and the sample composition. The detection limit is 1 ppm, operating range is from 1 ppm to 100% level concentrations, and repeatability is <0.5% relative standard deviation in peak area at constant temperature and pressure.

For the analysis of $\delta^{13}C_{CO2}$, carbon dioxide was cryogenically removed from the gas samples by liquid nitrogen and measured by Thermo Finnigan Delta ^{PLUS} XP isotope ratio mass spectrometer. Isotope ratios are given in the standard δ notation in permil (‰) versus VPDB (Vienna Pee Dee Belemnite). Errors for $\delta^{13}C$ are 0.5‰.

Noble gas isotopic ratios ($^3He/^4He$ and $^4He/^{20}Ne$) were measured from each gas sample that was inserted into the preparation line of the VG5400 noble gas mass spectrometer. The argon and the other chemically active gases (N_2, CO_2, etc.) were separated in a cryogenic cold system consisting of two cold traps and

Table 1
List of the Sites Investigated Including Location Names, Geographical Position (Geographical Coordinates in WGS84), Type of Manifestation (Mofetta, Bubbling Pool, and Drilling), Type of Sample (Free Gas), and Field Data (Temperature, pH, and EC Expressed in Microsiemens per Centimeter) Where Available

No.	Site	N	E	Type of manifestation	Sample type	*T* (°C)	pH	EC (μS/cm)
1	Torjai Stinky Cave	46.1198	25.9488	Mofetta	Free gas	nd	nd	nd
2	Timsós Cave	46.1191	25.9495	Mofetta	Free gas	nd	nd	nd
3	Gyilkos Cave	46.1218	25.9494	Mofetta	Free gas	nd	nd	nd
4	Buffogó peat bog pool	46.1279	25.9504	Bubbling pool	Free gas	1	3	472
5	Buffogó peat bog	46.1283	25.9504	Bubbling pool	Free gas	nd	nd	nd
6	Várpad-Ibolya pool	46.1134	25.9600	Bubbling pool	Free gas	7.1	6.46	3,220
7a	Bálványos mofetta	46.1118	25.9579	Bubbling pool	Free gas	9.7	4.99	3,722
7b	Bálványos mofetta	46.1118	25.9579	Bubbling pool	Free gas	9.7	4.99	3,722
8	Bálványos pool	46.1095	25.9590	Bubbling pool	Free gas	5	6.54	9,360
9	Csiszárfürdő-Iker pool white	46.1063	25.9514	Bubbling pool	Free gas	1.2	5.12	741
10	Csiszárfürdő-Hammas pool	46.1065	25.9504	Bubbling pool	Free gas	3.6	5.29	2,040
11	Csiszárfürdő-Timsós pool	46.1063	25.9504	Bubbling pool	Free gas	4.7	5.9	1,274
12	Csiszárfürdő-Csokoládés pool	46.1059	25.9508	Bubbling pool	Free gas	2.7	4.2	837
13	Mikesfürdő-Vallató pool	46.1170	25.9281	Bubbling pool	Free gas	5	6.16	2,300
14	Mikesfürdő-Vallató mofetta	46.1180	25.9283	Mofetta	Free gas	5	2.72	1,620
15	Mikesfürdő-Hammas pool	46.1168	25.9340	Bubbling pool	Free gas	1.9	2.96	968
16	Mikesfürdő-Bükkös pool	46.1161	25.9349	Bubbling pool	Free gas	2.3	3.6	584
17	Apor lányok feredeje-Small pool	46.1150	25.9496	Bubbling pool	Free gas	4.8	1.71	3,620
18	Apor lányok feredeje-spring on fault 2	46.1148	25.9496	Bubbling pool	Free gas	6.9	2.2	7,100
19	Apor lányok feredeje-Szemvíz 4	46.1148	25.9496	Bubbling pool	Free gas	4.2	2.6	2,080
20	Gyógyvizek	46.1133	25.9504	Bubbling pool	Free gas	3.7	1.85	2,780
21	Bálványos Sósmező drilling 1	46.1159	25.9424	Drilling	Free gas	nd	nd	nd
22	Bálványos Sósmező drilling 2	46.1159	25.9424	Drilling	Free gas	nd	nd	nd
23	Bálványos Sósmező drilling 3	46.1159	25.9424	Drilling	Free gas	nd	nd	nd
24	St Anna crater rim	46.1310	25.8936	mofetta	Free gas	nd	nd	nd
25	Jajdon pool	46.0701	25.9538	Bubbling pool	Free gas	4.6	7.3	1,489
26	Jajdon mofetta	46.0699	25.9538	Mofetta	Free gas	nd	nd	nd
27	Băile Tușnad mofetta	46.1421	25.8518	Mofetta	Free gas	nd	nd	nd
28	Lăzărești Nyírfürdő mofetta	46.1831	25.9520	Mofetta	Free gas	nd	nd	nd
29	Lăzărești Nyírfürdő pool	46.1831	25.9518	Bubbling pool	Free gas	6.6	5.96	768
30	Lăzărești Nyírfürdő pool 2	46.1829	25.9519	Bubbling pool	Free gas	nd	nd	nd
31	Ciucsângeorgiu mofetta	46.3363	25.9642	Mofetta	Free gas	nd	nd	nd

Note. EC = electrical conductivity; nd = not determined.

were adsorbed in an empty trap at 25 K. The Ne and He were adsorbed in a charcoal trap at 10 K. He was desorbed at 42 K and neon at 90 K and measured sequentially. The measurement procedure was calibrated with known air aliquots. The analytical uncertainties are 1% for He concentrations and 5% for Ne concentrations and 2.5% for $^3He/^4He$. $^3He/^4He$ ratio is expressed as R/R_a (being R_a the He isotope ratio of air and equal to $1.384 \cdot 10^{-6}$. He isotopic composition was corrected for the atmospheric He contamination (R/R_{ac}) considering the $^4He/^{20}Ne$ ratio; $R/R_{ac} = [R/R_a * (X - 1)]/(X - 1)$, where X is the air-normalized $^4He/^{20}Ne$ ratio taken as 0.318 (Sano & Wakita, 1985).

For the samples of the second analysis campaign, the chemical and isotopic composition of He-Ne and $^{13}C_{CO2}$ was determined in the laboratories of INGV-Palermo.

The concentrations of CO_2, CH_4, O_2, and N_2 were analyzed using an Agilent 7890B gas chromatograph with Ar as carrier and equipped with a 4-m Carbosieve S II and PoraPlot–U columns. A thermal conductivity detector was used to measure the concentrations of He, O_2, N_2, and CO_2 and a flame ionization detector for CO and CH_4. The analytical errors were 10% for He and 5% for O_2, N_2, CO, CH_4, and CO_2. More details on the analytical procedures used during this analysis are given in Liotta and Martelli (2012).

The carbon isotopic composition of CO_2 ($\delta^{13}C_{CO2}$) was determined using a Thermo Delta XP isotope ratio mass spectrometer equipped with a Thermo Scientific™ TRACE™ Ultra GC, and a 30-m Q-plot column (i.e., of 0.32 mm). The resulting $\delta^{13}C_{CO2}$ values are expressed in permil with respect to the international VPDB standard and analytical uncertainties are ±0.15‰. The method for the $\delta^{13}C$ determination of total

dissolved carbon is based on chemical and physical CO_2 stripping (Capasso et al., 2005). Isotopic ratios were measured using a Finnigan Delta Plus Mass Spectrometer. The results are expressed in permil of the international VPDB standard. The standard deviations of the $^{13}C/^{12}C$ ratios are ±0.2‰.

^3He, ^4He, and ^{20}Ne and the $^4He/^{20}Ne$ ratios were determined by separately inserting He and Ne into a split flight tube mass spectrometer (GVI-Helix SFT, for He analysis) and into a multicollector mass spectrometer (Thermo-Helix MC plus, for Ne analysis), after standard purification procedures (Rizzo et al., 2015). The analytical reproducibility was <0.1% for ^4He and ^{20}Ne. However, the estimation of He and Ne concentration agrees within 10% uncertainty respect to GC measurements. In this study, the time from sampling to analysis was lower than 2 weeks and results are fully reliable. The analytical error for He and Ne concentration measurements is generally below 0.3%.

3.2. Noble Gas Isotope Data for the Perşani Clinopyroxene

The chosen xenolith is a fresh spinel lherzolite with about 12% clinopyroxene content. Here we performed new noble gas analyses. The preparation, single-step crushing and analysis of fluid inclusions was the same as described by Correale et al. (2012) and references therein. Helium (^3He and ^4He) isotopes were measured separately by two different split-flight-tube mass spectrometers (Helix SFT-Thermo). The analytical uncertainty of the determination of the TGC (thermal conductivity detector) and the He and Ne abundances was ~10%. Error in the $^3He/^4He$ ratios is reported at the 1σ level.

4. Results

The site, sample names, and geographical locations with their GPS coordinates (WGS84, geographical coordinates), source type (mofettes or bubbling pools), temperature, pH, and electrical conductivity for bubbling pool samples are presented in Table 1, chemical and isotopic composition are listed in Tables 2 and 3. Noble gas isotopic compositions of clinopyroxenes from mantle xenoliths are shown in Table 4.

4.1. Chemical and Isotopic Composition of Gases

The CO_2 concentration in the collected gases ranges from 6.40% to 98.36%. Besides CO_2, H_2S (2.7×10^{-4} to 1.72×10^{-1}%), He (5.91×10^{-5} to 1.66×10^{-2}%), Ne (6.39×10^{-7} to 5.80x10^{-3}%), H_2 (1×10^{-5} to 2.3×10^{-1}%) CO (6×10^{-5} to 5×10^{-4}%), CH_4 (3.5×10^{-2} to 1.69%), N_2 (1.5×10^{-1} to 74.5%), and O_2 (2×10^{-3} to 18.99) are present in the gas samples. The ternary diagram $CO_2/50–N_2–O_2$ (Figure 3) shows a progressive enrichment in N_2 and O_2 of the samples, indicating a variable amount of air.

The $^3He/^4He$ ratios range between 0.77 and 3.10 R_a and the $^4He/^{20}Ne$ ratios from 0.36 to 1,700, which show that some of the collected gases are affected by air contamination (Table 3). The $^3He/^4He$ ratios after corrections for the air contamination (R/R_{ac}) are up to 3.25. The $\delta^{13}C_{CO2}$ ranges between −1.40‰ and −17.2‰ versus VPDB (Table 3).

4.2. Noble Gas Ratios of Fluid Inclusions From Persani Clinopyroxenes

Helium content in the fluid inclusions in clinopyroxenes ranged between 4.06×10^{-12} and 3.81×10^{-12} mol/g and Ne content between 2×10^{-15} and 2.74×10^{-15} mol/g, so the He/Ne ratios ranged between 1,390 and 2,030. The He isotopic signature in fluid inclusions was 5.95 Ra ± 0.01 (Table 4).

5. Discussion

5.1. Crustal Assimilation Versus Mantle Metasomatism

Helium comes from three different sources (mantle, crust, and air), which can be readily distinguished based on their characteristic isotopic ratios (Sano & Wakita, 1985). Helium isotopes are useful tracers for detecting deep fluids and their possible origin (crust, mantle, or atmosphere; Ozima & Podosek, 2002). It has been demonstrated that in the case of quiescent volcanoes, the active degassing of deep volatiles can occur for a long time after the last volcanic activity (Caracausi et al., 2009, 2015; Carapezza & Tarchini, 2007; Tassi et al., 2013).

The last eruption in Ciomadul occurred 30 ka (Harangi et al., 2010; Harangi, Lukács, et al., 2015; Molnár et al., 2019), yet there is an intense CO_2 degassing with a minimum flux of 8.7×10^3 t/year (Kis et al.,

Geochemistry, Geophysics, Geosystems

10.1029/2018GC008153

Table 2
Chemical Composition of the Different Gas Samples, Expressed in Percent

No.	Site	Campaign	Laboratory	H_2S	He	Ne	H_2	CO	CH_4	N_2	O_2	CO_2	Source
1	Torjai Stinky Cave	1st Campaign	Debrecen	nd	6.3×10^{-4}	3.5×10^{-5}	nd	nd	nd	nd	nd	nd	This work
	Torjai Stinky Cave		Rome	5.2×10^{-2}	7.0×10^{-4}	4.0×10^{-4}	2.0×10^{-5}		8.4×10^{-1}	1.6×10^{1}	4.9E+00	78.09	This work
	Torjai Stinky Cave	2nd Campaign	Palermo	1.8×10^{-2}	6.1×10^{-4}	6.4×10^{-7}	nd	5.0×10^{-4}	8.9×10^{-1}	1.2×10^{1}	2.9E+00	82.68	This work
2	Timsós Cave	1st Campaign	Debrecen	nd	6.9×10^{-4}	2.9×10^{-5}	nd	nd	nd	nd	nd	nd	This work
	Timsós Cave		Rome	6.8×10^{-2}	7.0×10^{-4}	3.0×10^{-4}	3.0×10^{-5}		8.4×10^{-1}	1.2×10^{1}	3.8E+00	83.05	This work
	Timsós Cave	2nd Campaign	Palermo	nd	6.3×10^{-4}	4.8×10^{-5}	nd	1.0×10^{-4}	9.3×10^{-1}	2.1E+00	7.3×10^{-2}	95.24	This work
3	Gyilkos Cave	1st Campaign	Debrecen	nd	5.6×10^{-4}	4.0×10^{-4}	nd	nd	nd	nd	nd	nd	This work
	Gyilkos Cave		Rome	nd	6.0×10^{-4}	1.0×10^{-3}	4.0×10^{-5}	nd	1.1×10^{-1}	3.8×10^{1}	9.5E+00	52.54	This work
4	Buffogó peat bog pool	1st Campaign	Debrecen	nd	6.7×10^{-4}	8.8×10^{-7}	nd	nd	nd	nd	nd	64.98	This work
	Buffogó peat bog pool		Rome	nd	8.0×10^{-4}	5.0×10^{-4}	4.0×10^{-5}	nd	9.7×10^{-1}	2.6×10^{1}	7.6E+00	64.98	This work
	Buffogó peat bog pool	2nd Campaign	Palermo	5.0×10^{-4}	7.1×10^{-4}	7.9×10^{-4}	nd	nd	1.3E+00	1.9E+00	1.5×10^{-1}	95.50	This work
5	Buffogó peat bog	1st Campaign	Debrecen	nd	9.4×10^{-4}	2.0×10^{-6}	nd	nd	nd	nd	nd	nd	This work
6	Várpad-Ibolya pool	1st Campaign	Debrecen	nd	5.9×10^{-5}	1.4×10^{-4}	nd	nd	nd	nd	nd	75.97	This work
	Várpad-Ibolya pool		Rome	nd	2.0×10^{-4}	5.0×10^{-4}	2.0×10^{-5}	nd	2.2×10^{-1}	1.8×10^{1}	5.7E+00	75.97	This work
7a	Bálványos mofetta	1st Campaign	Debrecen	nd	8.3×10^{-4}	1.8×10^{-6}	nd	nd	nd	nd	nd	nd	This work
7b	Bálványos mofetta	1st Campaign	Debrecen	nd	4.6×10^{-4}	1.8×10^{-4}	nd	nd	nd	nd	nd	94.87	This work
	Bálványos mofetta		Rome	nd	5.9×10^{-3}	4.1×10^{-3}	3.4×10^{-2}	nd	6.4×10^{-1}	3.7E+00	8.2×10^{-1}	94.87	This work
	Bálványos mofetta	2nd Campaign	Palermo	nd	1.0×10^{-3}	2.5×10^{-4}	1.4×10^{-3}	nd	1.3E+00	2.2×10^{1}	6.1E+00	68.25	This work
8	Bálványos pool	1st Campaign	Debrecen	nd	1.7×10^{-3}	1.7×10^{-4}	nd	nd	nd	nd	nd	63.84	This work
	Bálványos pool		Rome	nd	1.7×10^{-2}	5.8×10^{-3}	2.3×10^{-1}	nd	1.7E+00	2.6×10^{1}	8.4E+00	63.84	This work
9	Csiszárfürdő-Iker pool white	1st Campaign	Debrecen	nd	1.3×10^{-3}	1.0×10^{-5}	nd	nd	nd	nd	nd	nd	This work
	Csiszárfürdő-Iker pool white	2nd Campaign	Palermo	nd	9.5×10^{-4}	1.1×10^{-5}	nd	nd	1.7E+00	1.8E+00	1.7×10^{-1}	94.73	This work
10	Csiszárfürdő-Hammas pool	1st Campaign	Debrecen	nd	1.1×10^{-3}	6.4×10^{-7}	nd	nd	nd	nd	nd	96.72	This work
			Rome	1.1×10^{-1}	1.0×10^{-2}	2.3×10^{-3}	9.0×10^{-4}	nd	1.2E+00	9.8×10^{-1}	3.5×10^{-1}	96.72	this work
	Csiszárfürdő-Hammas pool	2nd Campaign	Palermo	nd	6.9×10^{-4}	5.5×10^{-6}	nd	nd	1.2E+00	8.8×10^{-1}	3.0×10^{-2}	94.81	This work
11	Csiszárfürdő-Timsós pool	1st Campaign	Debrecen	nd	1.1×10^{-3}	1.2×10^{-3}	nd	nd	nd	nd	nd	11.23	This work
	Csiszárfürdő-Timsós pool		Rome	nd	6.0×10^{-4}	1.0×10^{-3}	4.0×10^{-5}	nd	1.7×10^{-1}	7.0×10^{1}	1.9×10^{1}	11.23	This work
12	Csiszárfürdő-Csokoládés pool	1st Campaign	Debrecen	nd	9.4×10^{-4}	7.8×10^{-4}	nd	nd	nd	nd	nd	89.49	This work
	Csiszárfürdő-Csokoládés pool		Rome	1.7×10^{-2}	1.3×10^{-2}	4.6×10^{-3}	2.3×10^{-3}	nd	1.5E+00	7.4	1.6E+00	89.49	This work
	Csiszárfürdő-Csokoládés pool	2nd Campaign	Palermo	nd	8.7×10^{-4}	1.6×10^{-5}	nd	9.0×10^{-5}	1.5E+00	1.5E+00	1.4×10^{-1}	94.51	This work
13	Mikesfürdő-Vallató pool	1st Campaign	Debrecen	nd	4.5×10^{-4}	8.5×10^{-6}	nd	nd	nd	nd	nd	41.34	This work
	Mikesfürdő-Vallató pool		Rome	nd	5.9×10^{-3}	nd	6.0×10^{-4}	nd	5.5E-01	4.6×10^{1}	1.3×10^{1}	41.34	This work
	Mikesfürdő-Vallató pool	2nd Campaign	Palermo	nd	4.3×10^{-4}	1.4×10^{-5}	nd	nd	1.2E+00	1.8E+00	1.8×10^{-1}	93.95	This work
14	Mikesfürdő-Vallató mofetta	1st Campaign	Debrecen	nd	3.0×10^{-4}	4.0×10^{-5}	nd	nd	nd	nd	nd	91.86	This work
			Rome	2.7×10^{-2}	3.0×10^{-4}	2.0×10^{-4}	1.0×10^{-5}	nd	9.6×10^{-1}	5.2E+00	1.9E+00	91.86	This work

Geochemistry, Geophysics, Geosystems

10.1029/2018GC008153

Table 2 *(continued)*

No.	Site	Campaign	Laboratory	H_2S	He	Ne	H_2	CO	CH_4	N_2	O_2	CO_2	Source
	Mikesfürdő-Vallató mofetta												
15	Mikesfürdő-Hammas pool	1st Campaign	Debrecen	nd	7.2×10^{-4}	2.7×10^{-6}	nd	nd	nd	nd	nd	87.67	This work
	Mikesfürdő-Hammas pool		Rome	nd	7.0×10^{-4}	2.0×10^{-4}	4.0×10^{-5}	nd	9.9×10^{-1}	8.5E+00	2.9E+00	87.67	This work
	Mikesfürdő-Hammas pool	2nd Campaign	Palermo	nd	5.9×10^{-4}	7.9×10^{-6}	nd	nd	1.1E+00	1.1E+00	2.0×10^{-3}	94.83	This work
16	Mikesfürdő-Bükkös pool	1st Campaign	Debrecen	nd	8.0×10^{-4}	6.7×10^{-4}	nd	nd	nd	nd	nd	82.58	This work
	Mikesfürdő-Bükkös pool		Rome	nd	7.0×10^{-4}	4.0×10^{-4}	2.0×10^{-5}	nd	9.0×10^{-1}	1.3×10^{1}	4.0E+00	82.58	This work
	Mikesfürdő-Bükkös pool	2nd Campaign	Palermo	nd	7.7×10^{-4}	3.9×10^{-4}	nd	1.0×10^{-4}	1.1E+00	9.9E+00	2.4E+00	84.33	This work
17	Apor lányok feredeje-Small pool	1st Campaign	Debrecen	nd	1.2×10^{-3}	5.0×10^{-6}	nd	nd	nd	nd	nd	58.09	This work
	Apor lányok feredeje-Small pool		Rome	nd	8.0×10^{-4}	7.0×10^{-4}	3.0×10^{-5}	nd	7.7×10^{-1}	3.2×10^{1}	9.4E+00	58.09	This work
17	Apor lányok feredeje-Small pool	2nd Campaign	Palermo	2.7×10^{-4}	8.3×10^{-4}	6.5×10^{-5}	nd	9.0×10^{-5}	1.2E+00	1.1E+00	2.8×10^{-3}	97.15	This work
18	Apor lányok feredeje-spring on fault 2	1st Campaign	Debrecen	nd	7.8×10^{-4}	6.6×10^{-5}	nd	nd	nd	nd	nd	98.36	This work
	Apor lányok feredeje-spring on fault 2		Rome	1.7×10^{-1}	9.7×10^{-3}	2.2×10^{-3}	3.2×10^{-3}	nd	1.2E+00	1.5×10^{-1}	1.2×10^{-1}	98.36	This work
	Apor lányok feredeje-spring on fault 2	2nd Campaign	Palermo	3.5×10^{-4}	6.5×10^{-4}	7.8×10^{-7}	nd	nd	1.2E+00	8.6×10^{-1}	nd	96.38	This work
19	Apor lányok feredeje-Szemvíz 4	1st Campaign	Debrecen	nd	1.2×10^{-3}	2.8×10^{-6}	nd	nd	nd	nd	nd	36.24	This work
	Apor lányok feredeje-Szemvíz 4		Rome	2.0×10^{-2}	7.0×10^{-4}	1.0×10^{-3}	2.0×10^{-4}	nd	4.4×10^{-1}	5.0E+01	1.4×10^{1}	36.24	This work
	Apor lányok feredeje-Szemvíz 4	2nd Campaign	Palermo	nd	nd	nd	nd	6.0×10^{-5}	9.2×10^{-1}	2.0E+01	5.0E+00	74.99	This work
20	Gyógyvizek	1st Campaign	Debrecen	nd	8.1×10^{-4}	1.6×10^{-6}	nd	nd	nd	nd	nd	97.62	This work
	Gyógyvizek		Rome	1.1×10^{-1}	1.1×10^{-2}	2.6×10^{-3}	9.0×10^{-4}	nd	1.3E+00	5.3×10^{-1}	4.9×10^{-1}	97.62	This work
	Gyógyvizek	2nd Campaign	Palermo	nd	7.5×10^{-4}	8.6×10^{-4}	2.0×10^{-3}	1.5×10^{-4}	8.9×10^{-1}	1.4×10^{1}	3.5E+00	78.42	This work
21	Bálványos Sósmező drilling 1	1st Campaign	Debrecen	nd	2.6×10^{-4}	6.4×10^{-4}	nd	nd	nd	nd	nd	79.78	This work
	Bálványos Sósmező drilling 1		Rome	nd	2.0×10^{-4}	5.0×10^{-4}	3.0×10^{-5}	nd	3.5×10^{-2}	1.5×10^{1}	4.9E+00	79.78	This work
22	Bálványos Sósmező drilling 2	1st Campaign	Debrecen	nd	4.4×10^{-4}	5.4×10^{-4}	nd	nd	nd	nd	nd	80.62	This work
	Bálványos Sósmező drilling 2		Rome	nd	2.0×10^{-4}	4.0×10^{-4}	3.0×10^{-5}	nd	8.9×10^{-2}	1.5×10^{1}	4.6E+00	80.62	This work
23	Bálványos Sósmező drilling 3	1st Campaign	Debrecen	nd	6.2×10^{-4}	4.7×10^{-4}	nd	nd	nd	nd	nd	nd	This work
24	St Anna crater rim	1st Campaign	Debrecen	nd	8.2×10^{-4}	1.0×10^{-3}	nd	nd	nd	nd	nd	22.74	This work
	St Anna crater rim		Rome	nd	6.0×10^{-4}	1.0×10^{-3}	4.0×10^{-5}	nd	1.1×10^{-1}	6.1×10^{1}	1.6×10^{1}	22.74	This work
25	Jajdon pool	1st Campaign	Debrecen	nd	1.0×10^{-3}	1.1×10^{-3}	nd	nd	nd	nd	nd	20.50	This work

Geochemistry, Geophysics, Geosystems

10.1029/2018GC008153

Table 2 *(continued)*

No.	Site	Campaign	Laboratory	H_2S	He	Ne	H_2	CO	CH_4	N_2	O_2	CO_2	Source
	Jajdon pool		Rome	4.1×10^{-2}	8.6×10^{-3}	nd	4.0×10^{-4}	nd	4.0×10^{-1}	6.2×10^{1}	1.7×10^{1}	20.50	This work
26	Jajdon mofetta	1st Campaign	Debrecen	nd	5.9×10^{-4}	1.7×10^{-3}	nd	nd	nd	nd	nd	12.11	This work
	Jajdon mofetta		Rome	nd	5.8×10^{-3}	nd	5.0×10^{-4}	nd	1.3×10^{-1}	6.9×10^{1}	1.9×10^{1}	12.11	This work
27	Băile Tușnad mofetta	1st Campaign	Debrecen	nd	4.1×10^{-4}	3.2×10^{-4}	nd	nd	nd	nd	nd	97.97	This work
	Băile Tușnad mofetta		Rome	nd	4.1×10^{-3}	2.7×10^{-3}	7.0×10^{-4}	nd	5.9×10^{-1}	9.2×10^{-1}	5.2×10^{-1}	97.97	This work
28	Lăzărești Nyírfürdő mofetta	1st Campaign	Debrecen	nd	1.3×10^{-4}	2.0×10^{-5}	nd	nd	nd	nd	nd	97.99	This work
	Lăzărești Nyírfürdő mofetta		Rome	8.4×10^{-2}	2.2×10^{-3}	2.4×10^{-3}	2.0×10^{-4}	nd	7.8×10^{-1}	7.1×10^{-1}	4.3×10^{-1}	97.99	This work
29	Lăzărești Nyírfürdő pool	1st Campaign	Debrecen	nd	3.7×10^{-4}	9.7×10^{-4}	nd	nd	nd	nd	nd	93.14	This work
	Lăzărești Nyírfürdő pool		Rome	5.0×10^{-3}	3.7×10^{-3}	4.0×10^{-3}	1.4×10^{-3}	nd	1.3E+00	4.8E+00	7.3×10^{-1}	93.14	This work
	Lăzărești Nyírfürdő pool	2nd Campaign	Palermo	nd	1.1×10^{-4}	2.7×10^{-6}	nd	nd	8.1×10^{-1}	1.7E+00	5.0×10^{-2}	96.71	This work
30	Lăzărești Nyírfürdő pool 2	1st Campaign	Debrecen	nd	1.3×10^{-4}	2.7×10^{-5}	nd	nd	nd	nd	nd	97.66	This work
	Lăzărești Nyírfürdő pool 2		Rome	5.9×10^{-2}	1.9×10^{-3}	2.9×10^{-3}	9.0×10^{-4}	nd	7.9×10^{-1}	8.6×10^{-1}	6.2×10^{-1}	97.66	This work
31	Ciucsângeorgiu mofetta	1st Campaign	Debrecen	nd	5.9×10^{-4}	1.5×10^{-3}	nd	nd	nd	nd	nd	6.40	This work
	Ciucsângeorgiu mofetta		Rome	nd	5.4×10^{-3}	nd	5.0×10^{-4}	nd	6.4×10^{-2}	7.5×10^{1}	1.9×10^{1}	6.40	This work
32	Csiszárfürdő Băile Reci			nd	2.3×10^{-3}	2.3×10^{-3}	nd	nd	8.0×10^{-3}	nd	nd	99.99	Frunzeti, 2013
33	Gyógyvizek Izvoarele Tămăduitoare			nd	3.5×10^{-3}	4.6×10^{-6}	nd	nd	1.3E+00	1.4E+00	nd	97.24	Frunzeti, 2013
34	Apor lányok feredeje			nd	3.5×10^{-3}	1.3×10^{-6}	nd	nd	1.3E+00	1.9E+00	nd	96.76	Frunzeti, 2013
35	Torjai Büdös Cave (Stinky Cave)			nd	2.7×10^{-3}	4.6×10^{-6}	nd	nd	1.2E+00	2.1E+00	nd	96.80	Frunzeti, 2013
36	Mikesfürdő-Hammas			nd	3.3×10^{-3}	5.0×10^{-6}	nd	nd	1.3E+00	1.5E+00	nd	97.17	Frunzeti, 2013
37	Buffogó peat bog			nd	3.7×10^{-3}	1.4×10^{-6}	nd	nd	1.6E+00	1.6E+00	nd	96.80	Frunzeti, 2013
38	Tusnad			nd	5.3×10^{-5}	7.3×10^{-6}	nd	nd	3.0×10^{-3}	4.4E+00	nd	95.70	Frunzeti, 2013
39	Tusnad Nadas			nd	6.0×10^{-6}	nd	3.4×10^{-5}	nd	3.8×10^{-3}	3.2×10^{-1}	1.1×10^{-1}	99.56	Vaselli et al., 2002
40	Lăzărești Nyir			5.0×10^{-3}	7.8×10^{-4}	nd	4.0×10^{-5}	2.2×10^{-5}	3.4E+00	7.4E+00	1.4×10^{-2}	89.11	Vaselli et al., 2002
41	Sf Ana			nd	6.9×10^{-4}	nd	5.0×10^{-6}	7.0×10^{-6}	6.5×10^{-1}	1.6E+00	4.2×10^{-2}	97.69	Vaselli et al., 2002
42	Puturosul			1.2×10^{-2}	4.1×10^{-4}	nd	3.7×10^{-5}	nd	7.8×10^{-1}	9.0×10^{-1}	4.2×10^{-2}	98.26	Vaselli et al., 2002
43	Puturosul Sud			nd	1.4×10^{-3}	nd	9.0×10^{-6}	9.0×10^{-6}	2.4E+00	2.0E+00	3.0×10^{-2}	95.63	Vaselli et al., 2002
44	Bálványos			6.0×10^{-3}	6.3×10^{-4}	nd	1.5×10^{-4}	4.0×10^{-6}	1.1E+00	8.9×10^{-1}	4.4×10^{-2}	97.97	Vaselli et al., 2002
45	Torjai Büdös Cave (Stinky Cave)			nd	1.1×10^{-3}	nd	nd	nd	8.0×10^{-1}	9.7×10^{-1}	6.0×10^{-2}	98.20	Althaus et al., 2000
46	Apor lányok feredeje-Upper pool			nd	1.3×10^{-3}	nd	nd	nd	1.2E+00	1.5E+00	1.8×10^{-1}	97.75	Althaus et al., 2000

Table 2 *(continued)*

No.	Site	Campaign	Laboratory	H_2S	He	Ne	H_2	CO	CH_4	N_2	O_2	CO_2	Source
47	Apor lányok feredeje-Lower pool			nd	1.3×10^{-3}	nd	nd	nd	9.4×10^{-1}	7.3×10^{-1}	2.0×10^{-2}	98.16	Althaus et al., 2000
48	Bi × ad			nd	nd	nd	nd	nd	2.3×10^{-1}	8.9×10^{-1}	2.7×10^{-1}	99.00	Althaus et al., 2000
49	Bi × ad			nd	nd	nd	nd	nd	nd	nd	nd	nd	Althaus et al., 2000
50	Tusnad Nagy			nd	nd	nd	nd	nd	nd	nd	nd	nd	Althaus et al., 2000
51	Balvanyos Carpatii			nd	nd	nd	nd	nd	nd	nd	nd	nd	Althaus et al., 2000
52	Gyógyvízek			nd	nd	nd	nd	nd	nd	nd	nd	nd	Unpublished data
53	Bancu			nd	nd	nd	nd	1.0×10^{-5}	7.0×10^{-1}	2.4E+00	2.0×10^{-1}	95.88	Unpublished data
54	Lazaresti			nd	nd	nd	nd	nd	8.5×10^{-1}	2.0E+00	1.8×10^{-1}	96.4	Unpublished data

Note. nd = not determined.

2017), which is comparable to other dormant volcanic areas such as Panarea (1.72×10^4 t/year) and Roccamonfina (7.48×10^3 t/year) from Italy or Jefferson (7.92×10^3 t/year) from the United States.

In addition, previous investigations (Althaus et al., 2000; Vaselli et al., 2002; Túri et al., 2016) highlighted the outgassing of mantle-derived volatiles at Ciomadul volcano. He isotopic ratios in the fluids collected in this study are up to 3.1 R_a similar to those obtained from previous studies (Figure 4 and Table 3). These values are higher than those obtained from the surrounding areas such as in the Carpathian Foredeep and the Transylvanian Basin where He isotopic ratios are between 0.02 and 0.03 R_a (Baciu et al., 2017; Italiano et al., 2017; Vaselli et al., 2002, Figure 4). These latter values are typical of crustal fluids dominated by ^{4}He produced by decay of U and Th (e.g., Ozima & Podosek, 2002). The higher R_a values measured at Ciomadul could imply a higher contribution of magmatic He. Nevertheless, the 3.1 R_a value is significantly lower than the MORB and subcontinental lithospheric mantle (SCLM) value (Sano & Marty, 1995) requiring addition of radiogenic ^{4}He that decreased the pristine isotopic signature.

The mantle xenoliths of the Perşani volcanic field (approximately 40 km from the Ciomadul area) could provide the He isotopic signature of the lithospheric mantle beneath the region. The He isotopic ratios in fluid inclusions of the Persani clinopyroxenes are 5.95 ± 0.01 (Table 4), and these are lower than those of of previous measurements, from 6.5 to 7.3 R_a, obtained by Althaust et al. (1998) but consistent with the values of the SCLM ($R/R_a = 6.1 \pm 0.9$ R_a, Gautheron & Moreira, 2002). The continental crust ($R/R_a = 0.02$, Ozima & Podosek, 2002) and atmosphere ($R/R_a = 1$) have distinct isotopic values, and ^{4}He/^{20}Ne can be used to infer how mixing between the three possible end members can support the He isotopic signature of the fluids that outgass in the Ciomadul region (Figure 4). Most Ciomadul samples indicate a possible trend between air and a magmatic source, where the He ratio of the magmatic end member (3.1 R_a) is lower than that of the ECLM and the Perşani clinopyroxene. This is also supported by the trend line in the ^{3}He–CO_2–^{4}He ternary diagram (Figure 5), where the Ciomadul samples are along a trend showing variable amounts of CO_2 and R/R_{ac} values between 2 and 3. This trend reflects the dominance of radiogenic He in the fluids outgassing from the Ciomadul volcano. We have now to assess the possible processes that can add the radiogenic He component to the mantle component.

Such a relatively low He isotope ratio of the magma source is not uncommon in volcanic arc settings (e.g., Hilton et al., 1992; Allard et al., 1997; Martelli et al., 2004) and can be due to several processes involving the addition of radiogenically produced ^{4}He, such as magma aging, crustal assimilation, mixing between mantle, and crustal-derived fluids (Kennedy & van Soest, 2006; Torgersen et al., 1995). Unfortunately, there are no undifferentiated mantle-derived mafic rocks in the region of the Ciomadul volcano, so we cannot investigate the He isotope composition of the mantle directly below the volcano. In Ciomadul, only high-K dacitic volcanic products are found (Mason et al., 1996; Molnár et al., 2018, 2019; Vinkler et al., 2007), although occurrence of high-Mg minerals such as olivine and clinopyroxene in the dacites suggest involvement of primitive mafic magmas in the magma evolution of Ciomadul (Kiss et al., 2014; Vinkler et al., 2007).

Magma aging and crustal assimilation are two mechanisms that could account for the addition of the radiogenic He component to the mantle-derived melts. Both these processes have been invoked to explain low He isotopic ratios (<MORB and SCLM) in different volcanic regions, worldwide, such as Aeolian Island, Italy (Mandarano et al., 2016), and Iceland (Condomines et al., 1983). The magma-aging mechanism considers an addition of ^{4}He by radiogenic decay in the magma itself.

Table 3
Isotopic Composition of the Gas Samples

No.	Site	Campaign	Laboratory	R/Ra measured	R/Ra corrected	4He/ 20Ne	δ^{13} C–CO_2	δ18 O–CO_2	CO_2/3He	Source
1	Torjai Stinky Cave	1st Campaign	Debrecen	2.67	2.69	18.07	−3.24	−6.74	3.29E+10	This work
		2nd Campaign	Palermo	3.01	3.01	955.55	−3.09	nd	3.24E+10	This work
2	Timsós Cave	1st Campaign	Debrecen	2.71	2.73	23.83	−3.36	−6.08	3.17E+10	This work
		2nd Campaign	Palermo	2.90	2.95	13.20	−3.47	nd	3.69E+10	This work
3	Gyilkos Cave	1st Campaign	Debrecen	2.12	2.40	1.40	−3.22	−6.63	nd	This work
4	Buffogó peat bog pool	1st Campaign	Debrecen	2.86	2.86	758.43	−2.70	−9.00	2.45E+10	This work
		2nd Campaign	Palermo	2.27	2.95	0.90	−3.15	nd	3.27E+10	This work
5	Buffogó peat bog	1st Campaign	Debrecen	1.78	1.78	477.09	nd	nd	nd	This work
6	Várpad-Ibolya pool	1st Campaign	Debrecen	1.49	2.43	0.44	−3.13	nd	3.81E+11	This work
7a	Bálványos mofetta	1st Campaign	Debrecen	1.13	1.13	456.45	nd	nd	nd	This work
7b	Bálványos mofetta	1st Campaign	Debrecen	2.06	2.19	2.62	−4.20	nd	6.71E+10	This work
		2nd Campaign	Palermo	2.06	2.15	4.0	−17.20	nd	nd	This work
8	Bálványos pool	1st Campaign	Debrecen	2.14	2.17	9.75	−2.84	nd	1.26E+10	This work
9	Csiszárfürdő-Iker pool white	1st Campaign	Debrecen	2.43	2.44	127.86	−3.06	−7.44	nd	This work
		2nd Campaign	Palermo	2.81	2.82	90.4	nd	nd	2.53E+10	This work
10	Csiszárfürdő-Hammas pool	1st Campaign	Debrecen	1.97	1.97	1695.21	−3.59	−8.40	3.23E+10	This work
10		2nd Campaign	Palermo	2.90	2.90	123.8	−3.20	nd	3.43E+10	This work
11	Csiszárfürdő-Timsós pool	1st Campaign	Debrecen	2.46	3.09	0.95	−2.47	nd	2.33E+09	This work
12	Csiszárfürdő-Csokoládés pool	1st Campaign	Debrecen	2.44	2.90	1.21	−3.40	nd	2.37E+10	This work
12		2nd Campaign	Palermo	2.90	2.91	55.00	−2.60	nd	2.68E+10	This work
13	Mikesfürdő-Vallató pool	1st Campaign	Debrecen	2.72	2.73	52.98	−2.28	−6.87	2.42E+10	This work
13		2nd Campaign	Palermo	2.55	2.57	31.4	−2.30	nd	6.18E+10	This work
14	Mikesfürdő-Vallató mofetta	1st Campaign	Debrecen	2.21	2.25	7.43	−2.45	−6.37	9.87E+10	This work
15	Mikesfürdő-Hammas pool	1st Campaign	Debrecen	2.74	2.74	266.70	−3.35	−7.09	3.19E+10	This work
15	l	2nd Campaign	Palermo	3.02	3.03	74.0	−2.90	nd	3.85E+10	This work
16	Mikesfürdő-Bükkös pool	1st Campaign	Debrecen	2.46	2.93	1.19	−2.65	nd	2.52E+10	This work
16		2nd Campaign	Palermo	1.98	2.16	2.0	−3.20	nd	3.64E+10	This work
17	Apor lányok feredeje-Small pool	1st Campaign	Debrecen	1.99	1.99	233.48	−3.09	−5.13	1.81E+10	This work
17		2nd Campaign	Palermo	2.81	2.86	12.8	nd	nd	2.95E+10	This work
18	Apor lányok feredeje-spring on fault 2	1st Campaign	Debrecen	3.10	3.15	11.80	−3.85	nd	2.87E+10	This work
18		2nd Campaign	Palermo	2.90	2.90	836.3	−4.00	nd	3.68E+10	This work
19	Apor lányok feredeje-Szemvíz 4	1st Campaign	Debrecen	1.85	1.85	425.84	−3.52	−2.79	1.20E+10	This work
19		2nd Campaign	Palermo	1.34	1.50	1.00	−2.60	nd	nd	This work
20	Gyógyvizek	1st Campaign	Debrecen	2.73	2.73	497.01	−3.42	−4.58	3.17E+10	This work
20		2nd Campaign	Palermo	1.46	1.73	0.9	−3.30	nd	4.37E+10	This work
21	Bálványos Sósmező drilling 1	1st Campaign	Debrecen	0.78	0.27	0.41	−4.61	−5.44	8.13E+11	This work
22	Bálványos Sósmező drilling 2	1st Campaign	Debrecen	0.82	0.72	0.82	−4.37	−5.30	1.82E+11	This work
23	Bálványos Sósmező drilling 3	1st Campaign	Debrecen	2.43	2.83	1.32	−3.92	nd	nd	This work
24	St Anna crater rim	1st Campaign	Debrecen	1.99	2.58	0.78	−2.80	−9.05	7.78E+09	This work
25	Jajdon pool	1st Campaign	Debrecen	2.30	2.83	0.99	−3.41	nd	5.02E+09	This work
26	Jajdon mofetta	1st Campaign	Debrecen	1.45	3.25	0.36	−3.96	nd	4.51E+09	This work
27	Băile Tuşnad mofetta	1st Campaign	Debrecen	2.02	2.32	1.28	−1.50	nd	7.48E+10	This work
28	Lăzăreşti Nyírfürdő mofetta	1st Campaign	Debrecen	1.43	1.45	6.50	−2.08	nd	3.84E+11	This work
29	Lăzăreşti Nyírfürdő pool	1st Campaign	Debrecen	1.11	1.46	0.38	−1.40	nd	1.24E+11	This work
29		2nd Campaign	Palermo	1.01	1.01	40.2	−1.50	nd	6.45E+11	This work
30	Lăzăreşti Nyírfürdő pool 2	1st Campaign	Debrecen	1.30	1.32	4.69	−1.91	nd	4.13E+11	This work
31	Ciucsângeorgiu mofetta	1st Campaign	Debrecen	0.77	0.14	0.39	−2.95	nd	5.50E+10	This work
32	Csiszárfürdő Băile Reci			0.796	0.796	0.99	nd	nd	3.89E+10	Frunzeti, 2013
33	Gyógyvizek Izvoarele Tămăduitoare			2.302	2.302	766.09	−3.25	−7.43	8.62E+09	Frunzeti, 2013
34	Apor lányok feredeje			2.438	2.438	2686.92	−3.72	−4.92	8.17E+09	Frunzeti, 2013
35	Torjai Büdös Cave (Stinky Cave)			2.199	2.199	583.84	−3.15	−7.48	1.17E+10	Frunzeti, 2013
36	Mikesfürdő–Hammas			2.242	2.242	656.89	−3.16	−9.87	9.47E+09	Frunzeti, 2013
37	Buffogó peat bog			2.274	2.274	2711.03	−2.77	−9.21	8.31E+09	Frunzeti, 2013
38	Tusnad			0.724	0.724	9.79	−4.7	−8.2	1.79E+12	Frunzeti, 2013

Table 3 *(continued)*

No.	Site	Campaign	Laboratory	R/Ra measured	R/Ra corrected	4He/ 20Ne	δ^{13} C–CO_2	δ18 O–CO_2	CO_2/3He	Source
39	Tusnad Nadas			1.66	1.66	1.28	−4.42	nd	7.19E+12	Vaselli et al., 2002
40	Lăzărești Nyir			2.95	2.95	7.7	nd	nd	2.79E+10	Vaselli et al., 2002
41	Sf Anna			3.18	3.18	25	nd	nd	3.20E+10	Vaselli et al., 2002
42	Puturosul			2.29	2.29	10.11	nd	nd	7.53E+10	Vaselli et al., 2002
43	Puturosul Sud			nd	nd	nd	−4.7	nd	nd	Vaselli et al., 2002
44	Bálványos			4.48	4.48	163	nd	nd	2.52E+10	Vaselli et al., 2002
45	Torjai Büdös Cave (Stinky Cave)			3.1	3.100	47.3	nd	nd	2.07E+10	Althaus et al., 2000
46	Apor lányok feredeje-Upper pool			3.12	3.120	151	nd	nd	1.72E+10	Althaus et al., 2000
47	Apor lányok feredeje-Lower pool			3.19	3.190	712	nd	nd	1.70E+10	Althaus et al., 2000
48	Bixad			1.47	1.470	0.67	nd	nd	nd	Althaus et al., 2000
49	Bixad			0.8	0.8	1.3	nd	nd	nd	Althaus et al., 2000
50	Tusnad Nagy			1.2	1.2	6.44	nd	nd	nd	Althaus et al., 2000
51	Balvanyos Carpatii			3.04	3.04	1.06	nd	nd	nd	Althaus et al., 2000

Note. $^3He/^4He$ ratios are normalized to the atmosphere and listed as R/R_a values corrected for the atmospheric He contamination (R/R_{ac}) considering the $^4He/^{20}Ne$ ratio; $\delta^{13}C–CO_2$ and $\delta^{18}O–CO_2$ are expressed in permil versus Vienna Pee Dee Belemnite. nd = not determined.

In constrast, crustal assimilation furnishes ^4He by interaction between magma and the whole rock. First, we investigated the likelihood that the magma aging model can interpret the low He isotopic signature in the fluids that outgas at Ciomadul volcano.

The $^3He/^4He$ ratio of the fluid inclusions of the Persani clinoproxene (5.95 $R_a \pm 0.01$) can be assumed to represent the mantle end member value beneath of the region. Thus, the primary magmas of Ciomadul could be also characterized by such isotope ratio. The Ciomadul dacites have U and Th concentrations of 3 and 15 ppm, respectively (Molnár et al., 2018, 2019; Vinkler et al., 2007). Using these data, the magma-aging model calculation yield $^3He/^4He$ ratio around 4.65 R_a after 30 kyr (Figure 6). Thus, this process alone cannot be responsible for the low He (approximately 3.1 R_a) isotopic signature of the Ciomadul fluids. Furthermore, if we assume the U (1.5 ppm) and Th (5.5 ppm) contents of the Persani basalts (Harangi et al., 2013), the magma-aging model is still not a viable process to provide the required ^4He addition and generate the low $^3He/^4He$ for Ciomadul gases.

The relatively low He isotopic ratio can also be explained by high-level crustal assimilation (e.g., van Soest et al., 2002), which has to also be evaluated. Assuming the U and Th amount of the typical upper crust, 2.7 and 10.5 ppm, respectively (Rudnick & Gao, 2003), and an age of 5 Ma, 3% of crustal assimilation could be sufficient to achieve the observed low He isotopic ratios. The Sr–Nd–O isotope compositions of the erupted magmas sensitively reflect such a process. Mason et al. (1996) published isotopic data for three samples of the Ciomadul volcanic system. They have distinct isotopic features compared to the calc-alkaline volcanic suite of the Calimani-Gurghiu-Harghita chain. Although the Sr–Nd isotopic data could suggest an assimilation and fractional crystallization process with 10–35% assimilation of flysch sediment, such a high crustal contamination is not feasible, based on the fairly low $\delta^{18}O$ values (6.3–7.1‰) of the phenocrysts from the dacites (Mason et al., 1996). Instead, they suggested that these isotopic characteristics could also be explained by source contamination from subduction-related fluids. In fact, the bulk-rock composition of the Ciomadul dacites has unique characteristics with high Sr, Ba (both showing typically >1,000 ppm),

Table 4
Isotopic Composition of Persani Clinopyroxene

Sample	He (mol/g)	Ne (mol/g)	He/Ar	$^4He/^{20}Ne$	R/R_a	R/R_{ac}
Cpx xenolith	4.06E-12	2.00E-15	0.92	2030.46	5.96	5.96
Cpx xenolith 2	3.81E-12	2.74E-15	0.91	1389.41	5.94	5.94

Note. $^3He/^4He$ ratios are normalized to the atmosphere and listed as R/R_a values ($R = {}^3He/{}^4He$ isotopic ratio of the sample, R_a = atmospheric $^3He/^4He = 1.382 \times 10^{-6}$) and corrected for the atmospheric helium contamination (R/R_{ac}) considering the $^4He/^{20}Ne$ ratio.

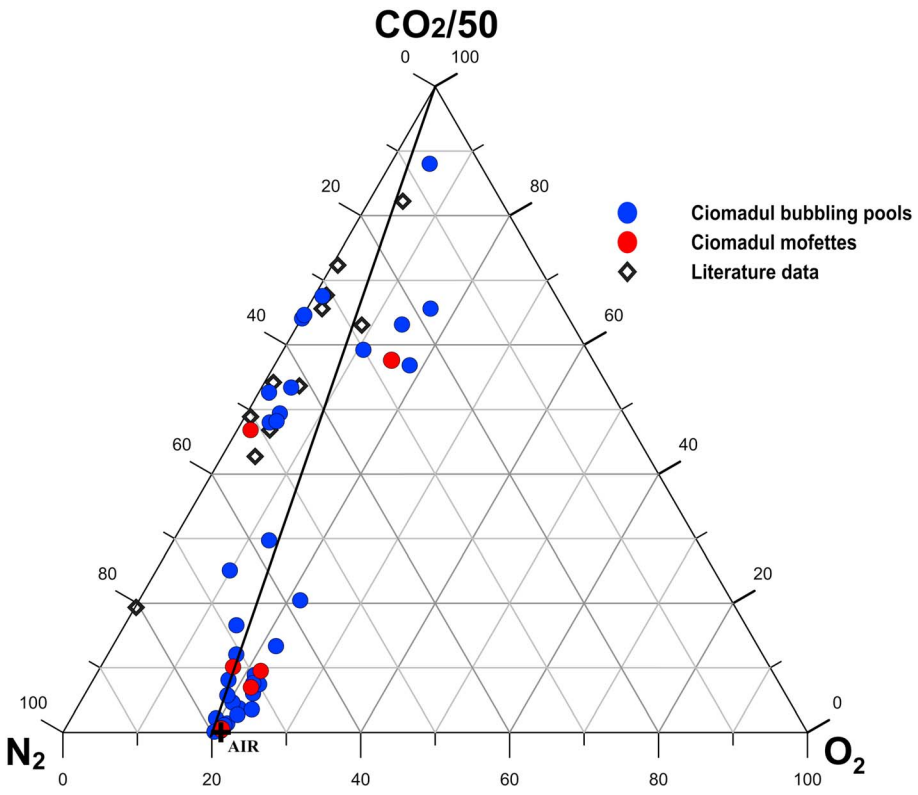

Figure 3. $CO_2/50$–O_2–N_2 triangular diagram showing the relative contents of components. The samples distribution highlights mixing between CO_2 and atmospheric gas species. Literature data from Ciomadul area are represented by data from Althaus et al., 2000, Frunzeti, 2013, and Vaselli et al., 2002).

and high K compositions and low concentrations of heavy rare Earth elements (Molnár et al., 2018, 2019; Seghedi et al., 1987; Vinkler et al., 2007). Furthermore, the high-Mg pargasitic amphiboles thought to have derived from the less differentiated magmas have also relatively high Ba content (Kiss et al., 2014). Thus, these peculiar compositional characters can be due to the nature of the magma source rather than magma differentiation processes. The elevated K, Sr, and Ba contents of the assumed mantle source of the Ciomadul primary magmas can be due to metasomatism, and this is in contrast what the peridotite xenoliths from the Persani volcanic field show (Vaselli et al., 1995). In fact, the He signature of the outgassed volatiles at Ciomadul resembles the values in fluids from other subduction-related volcanic systems (i.e., Italy, and Indonesia; Hilton et al., 1992; Martelli et al., 2004), where the mantle source regions seem to be contaminated by crustal material that added radiogenic ^{4}He and decreased the pristine He isotopic signature (Hilton et al., 2002).

Such a small-scale spatial heterogenity of the lithospheric mantle beneath this area can be explained by the closer location of Ciomadul to the collision front, where subduction is expected to have occurred during the Miocene up to around 11 Ma (Cloetingh et al., 2004; Mațenco et al., 2007; Royden et al., 1982; Seghedi et al., 2011). Such a scenario is not unique; Martelli et al. (2004) suggested that the relatively low He isotopic ratio in the volcanic rocks of Central Italy can be explained by magma source features (i.e., contribution of radiogenic He from metasomatic, subduction-related fluids and ingrowth of ^{4}He in the lithospheric mantle). We note that the $^{87}Sr/^{86}Sr$ isotopic ratio of the Ciomadul dacites and the highest $^3He/^4He$ isotopic values of the emitted gases plot into the same trend (Figure 5 in Martelli et al., 2004) what the Central Italian volcanic areas form.

In summary, considering the petrology of the Ciomadul volcanic products, the relatively low He isotope magmatic end member of the Ciomadul gases can be interpreted as due to magma-source characteristics, where the radiogenic He was added via subduction-related fluids and increased radioactive ingrowth following the metasomatism. However, a mixing between mantle-derived fluids with and SCLM He isotopic

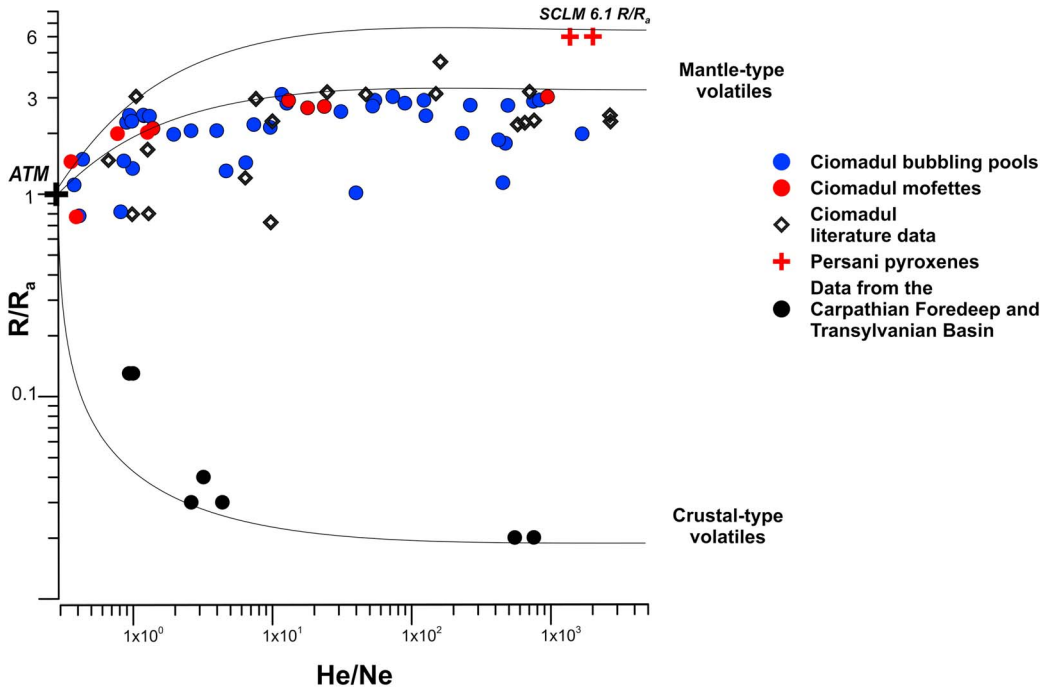

Figure 4. Helium isotopic ratios (R/R_a values) and $^4He/^{20}Ne$ relationships. The theoretical lines represent binary mixings of atmospheric He with mantle-originated and crustal He (Pik & Marty, 2008). The assumed end members for He-isotopic ratios and $^4He/^{20}Ne$ ratios are ATM (1 R_a, He/Ne = 0.318, Sano & Wakita, 1985); subcontinental European mantle is 6.1 ± 0.9 R_a and $^4He/^{20}Ne$ ratio = 1,000 (Gautheron & Moreira, 2002); typical crustal end member is 0.02 R_a and $^4He/^{20}Ne$ ratio = 1,000 (Sano & Marty, 1995). Literature data for comparison: data after Althaus et al. (2000), Baciu et al. (2007, 2017), Frunzeti (2013), and Vaselli et al. (2002). SCLM = subcontinental lithospheric mantle.

signature and ^{4}He-rich crustal fluids coming from shallow crustal layers should still be further explored as a possible process responsible of the low He isotopic ratios in the Ciomadul fluids. This likelihood will be discussed in the next section.

5.2. Sources and Origin of Carbon Dioxide

The carbon isotopic composition of CO_2 ($\delta^{13}C_{CO2}$) from the studied fluids range between −1.40‰ and −4.61‰ versus VPDB, consistent with previous measurements in the area (−2.77‰ to −4.70‰; Frunzeti, 2013; Sarbu et al., 2018; Vaselli et al., 2002). In the Pannonian Basin (Central Europe), the carbon isotopic composition of CO_2 gases shows values in a narrow range between −3‰ and −7‰ with an average value of −5‰ VPDB based on hundreds of measurements (Bräuer et al., 2016; Cornides, 1993; Palcsu et al., 2014; Sherwood-Lollar et al., 1997). These values are consistent with a mantle origin. In contrast, crustal-derived CO_2 is characterized by a $\delta^{13}C$ of about −25‰ in case of biogenic sedimentary source and around 0‰ considering thermometamorphism of limestone (Sano & Marty, 1995 and references therein). The Ciomadul gases overlap the range of mantle composition, even if some samples have more positive values that cannot be explained by the addition of a crustal biogenic component (Table 3 and Figures 7 and 8). To constrain the origin of CO_2 in the fluids emitted by the Ciomadul volcano, we used the relationship between the elemental ratio $CO_2/^3He$ and the isotopic signature $\delta^{13}C_{CO2}$ (Sano & Marty, 1995; Figure 7).

The $CO_2/^3He$ ratios of the Ciomadul gases are higher than 2×10^9, the expected mantle ratio (Marty & Jambon, 1987) and which suggests an addition of a crustal component. It is interesting that these ratios fall into the same trend as shown by volcanic and fumarolic gases measured at volcanic arcs, worldwide (Mason et al., 2017; Figures 8a and 8b). Almost all the Ciomadul samples fall close the mixing line between a mantle component and a limestone end member suggesting that mixing of the two sources could be the main process that controls the CO_2–^3He systematics in these fluids. In contrast, CO_2 fluids in the Transylvanian Basin, (Baciu et al., 2007, 2017) west of the volcano have distinct character and fall closer to the mantle-organic sediment mixing line. Rayleigh-type fractionation due to gas exsolution from water is not a

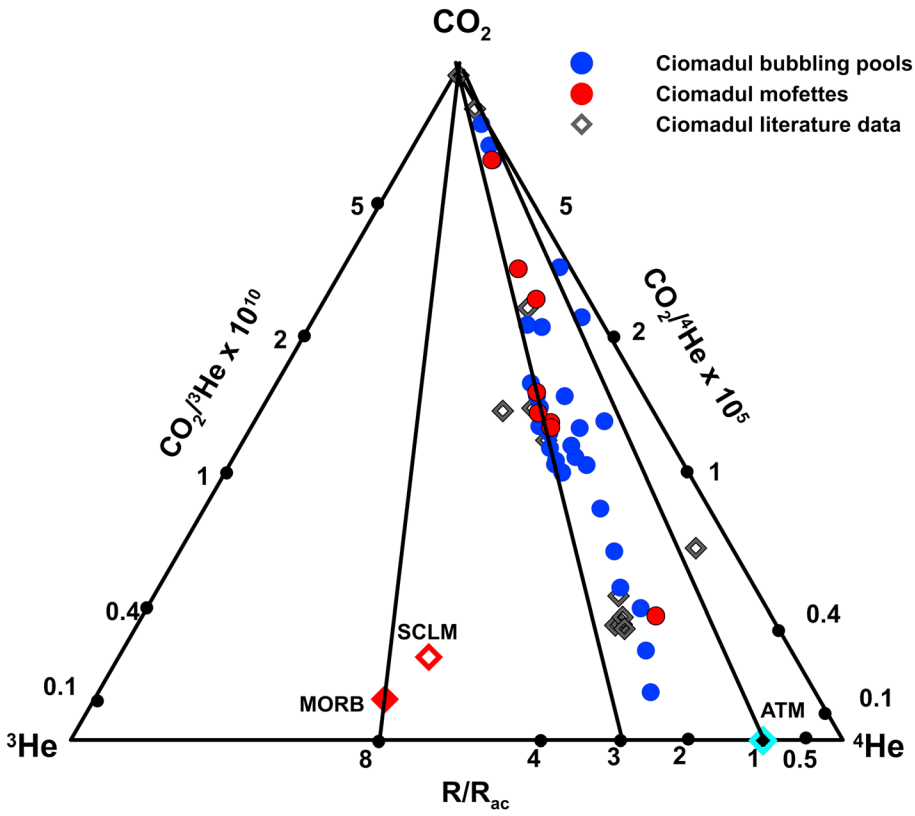

Figure 5. Ternary CO_2–^{3}He–^{4}He diagram of Ciomadul gas samples. Ciomadul literature data after Althaus et al. (2000), Frunzeti (2013) and Vaselli et al. (2002). For reference, we have plotted the MORB (Marty & Jambon, 1987) and SCLM values (Gautheron & Moreira, 2002). SCLM = subcontinental lithospheric mantle.

plausible process to produce the carbon isotopic signature and the $CO_2/^3He$ of the studied fluids (Figure 7; Holland & Gilfillan, 2013; Roulleau et al., 2015). However, the $^{13}C_{CO2}$ values of most of the samples fall in the narrow range of −2‰ and −5‰, which is a typical signature for mantle-derived carbon. We obtain the same trend in the He isotopic ratios (R/R_a) versus $^{13}C_{CO2}$ (VPDB) plot (Figures 8a and 8b), where the Ciomadul samples clearly approach the mantle end member and overlap the isotopic values of many other volcanic systems related to subduction areas. Remarkably the Ciomadul samples show similarities in He–C isotopic composition with active and dormant volcanic regions (e.g., Italy and Indonesia).

The involvement of carbonatic component can be explained by mixing with fluids derived from thermometamorphic decomposition of carbonates in the flysch sedimentary pile or by mantle source contamination via subducted carbonatic material. The mantle source of the Ciomadul magmas is considered to be a metasomatic lithospheric mantle based on the compositional features of the dacitic rocks. The relatively low He isotopic ratio can be due to these source characteristics, whereas metasomatism was the result of slab-derived fluids during the Miocene subduction along the Eastern Carpathians followed by ingrowth of radiogenic He by radioactive decay. The Sr–Nd–O isotope data of the volcanic rocks do not support significant upper-level crustal contamination but rather crustal component addition to the source region via slab-derived fluid metasomatism (Mason et al., 1996). The combination of He and C isotopic data suggests that this crustal component consisted of decomposed subducted carbonate material as suggested also for the volcanic rocks in Italy, although addition of fluids from carbonate decomposition at shallow crustal level cannot be unambiguously excluded.

5.3. Relationship With the Deep Magmatic System

Dormant volcanoes pose a particular hazard to society since there is much less awareness about a possible eruption event. However, the scientific community is giving increased attention to these volcanoes and

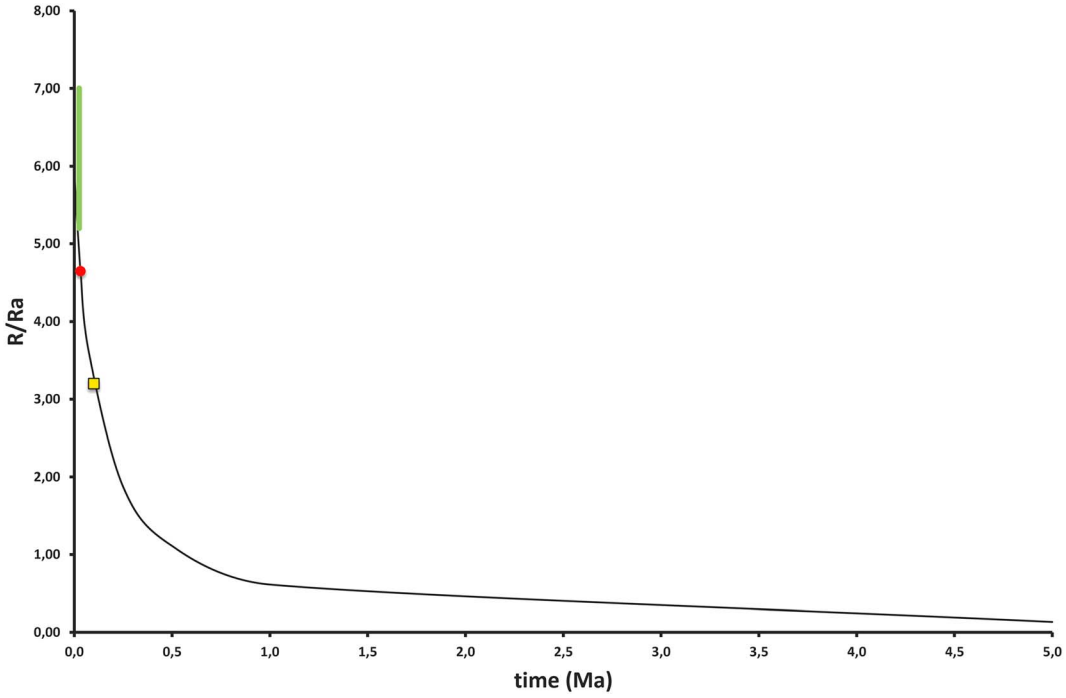

Figure 6. Magma aging evolution over time of the He isotopic signature (as R/R_a). The green bar is the range of the subcontinental lithospheric mantle He isotopic ratio (6.1 ± 0.9; Gautheron & Moreira, 2002). The red circle is the value or the $^3He/^4He$ (4.65 R_a) at 30 ka for the magma aging evolution. $^3He/^4He = 3.2$ is at 100 ka (yellow square).

the surrounding areas that are generally characterized by intense gas emissions (Burton et al., 2013, and references therein). Recent investigations highlighted the presence of an active plumbing system even below volcanoes which last erupted >10 kyr (e.g., Colli Albani, Italy; Trasatti et al., 2018; Uturuncu, Bolivia; Sparks et al., 2008; Comeau et al., 2015; Tatun, Taiwan; Konstantinou et al., 2007; Lin & Pu, 2016). Harangi, Novák, et al. (2015) suggested the term PAMS volcano, that is, volcano with potentially active magma storage for these long-dormant volcanoes, which have clear implication for a subvolcanic melt-bearing magma plumbing system. Ciomadul belongs to this category, since there are a number of observations suggesting that a melt-bearing magma body could still exist beneath it (Harangi, Novák, et al., 2015; Popa et al., 2012; Szakács & Seghedi, 2013). The isotopic composition of the emitted gases coupled to the high localized heat flow in the area of the Ciomadul vocano gives additional support to this interpretation.

This involves the similarities in the isotope composition of CO_2 and He of the gases emitted at the Ciomadul with those found in other active and dormant volcanic arc systems worldwide and their proposed high magmatic component. Furthermore, the Ciomadul volcanic system is characterized by relatively high CO_2 gas fluxes (Kis et al., 2017). This is consistent with the presence of a still-degassing magma below the Ciomadul system as inferred by geophysical investigations that recognized a low-resistivity and low-velocity anomaly in the crust, below the volcano (Harangi, Novák, et al., 2015; Popa et al., 2012) as well as petrologic observations suggesting the involvement of a mafic magma in the petrogenesis of the erupted dacite (Kiss et al., 2014). The measurements of U–Th and U–Pb spot ages on zircons suggest a long-standing magma storage that could go back as far as about 350 ka (Harangi, Lukács, et al., 2015; Lukács et al., 2018). Molnár et al. (2018, 2019) presented a detailed eruption chronology for the Ciomadul lava dome field involving the Ciomadul volcanic complex and emphasized that volcanic activity could be renewed even after long (>100 kyr) repose times. Several tens-of-kiloyears quiescence periods between the active phases have also been pointed out also during the evolution of the Ciomadul volcanic complex (Harangi, Lukács, et al., 2015; Molnár et al., 2019). However, the zircon U–Th and U–Pb ages suggest that crystallization was ongoing also during the long quiescence periods, that is, there was an active magma storage beneath the apparently inactive volcano This suggests a long-standing felsic upper-crustal crystal mush system underlain by a mafic

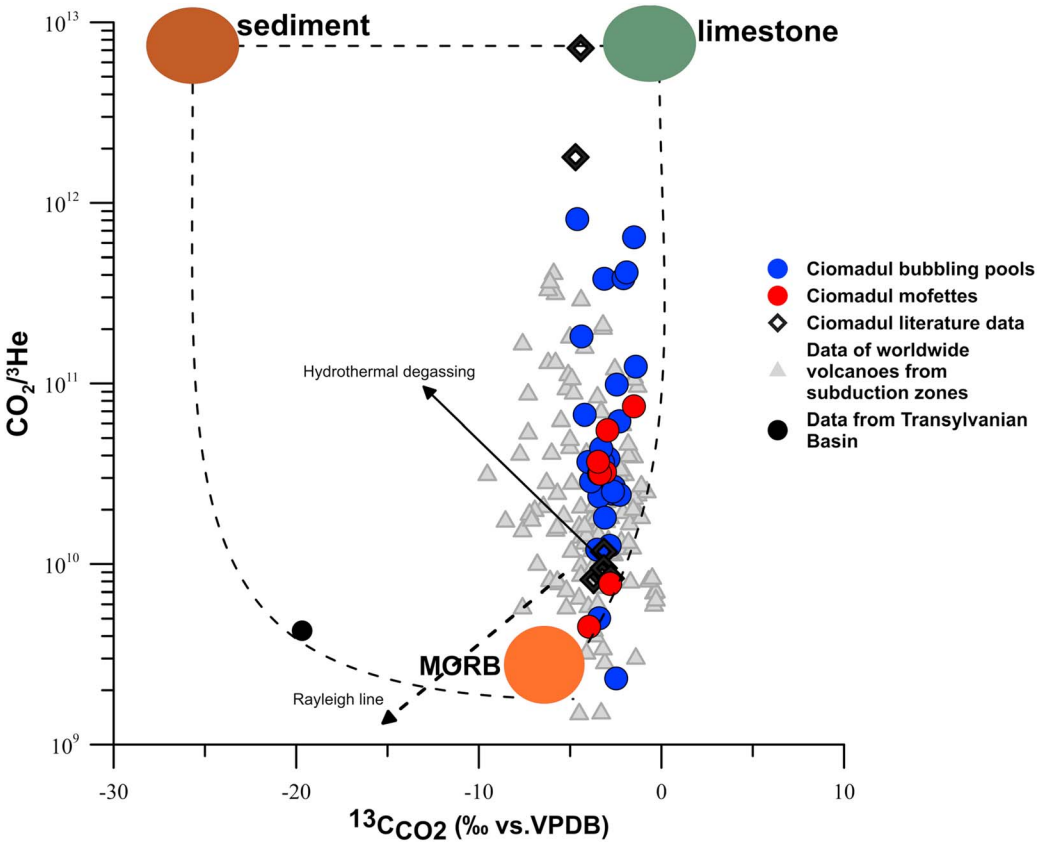

Figure 7. Correlation diagram of Sano & Marty (1995) plotting $CO_2/^3He$ versus $^{13}C_{CO2}$ (VPDB) of Ciomadul gas emissions. Lines show the theoretical mixing between a mantle end member and a crustal end member represented by marine limestone and organic sediment carbon. Ciomadul samples are showing a trend of mixing between fluids of mantle origin and fluids originating from limestone. Literature data for comparison: data after Althaus et al. (2000), Baciu et al. (2007, 2017), and Frunzeti et al. (2013) and Vaselli et al. (2002). Data on individual volcanoes worldwide are based on the compilation of Mason et al. (2017), by Allard (1983), Marty and Giggenbach (1990), Poorter et al. (1991), Varekamp et al. (1992), Sturchio et al. (1993), Sano et al. (1994), Sano and Marty (1995), Tedesco et al. (1995), Hilton (1996), Sano and Williams (1996), Allard et al. (1997), Fischer et al. (1998), van Soest et al. (1998), Pedroni et al. (1999), Lewicki et al. (2000), Parello et al. (2000), Favara et al. (2001), Snyder et al. (2001), Shaw et al. (2003), Symonds et al. (2003), Jaffe et al. (2004), Capasso et al. (2005), Carapezza et al. (2007), de Leeuw et al. (2007), Werner et al. (2009), Capaccioni et al. (2011), Tassi et al. (2011), Aguilera et al. (2012), Melián et al. (2012), and Caracausi et al. (2013).

hot zone in the lower crust, as has already been suggested by petrologic interpretations (Kiss et al., 2014). The diverse amphibole compositions in the dacites are consistent with a polybaric magma evolution, that is, with transcrustal magma storage (Cashman et al., 2017; Sparks & Cashman, 2017) comprising ephemeral melt-dominated bodies, that is, magma chambers at various depths. In addition, fluid-gas accumulation zones can also have developed within this magma storage (Christopher et al., 2015; Sparks & Cashman, 2017). Thus, a possible source of the CO_2 gases could be these fluid entrapment zones within the crystal mush during quiescent period. However, gas emission is more common around the Ciomadul volcanic complex and significantly lower within the volcano itself (Kis et al., 2017). Allard et al. (1991), and Edmonds (2008) pointed out that stronger degassing around the volcanic edifice is not uncommon in volcanic regions. An alternative source of the CO_2 gases could be mafic magma residing at deeper level, possibly at the lower crust. Indeed, the occurrence of high-Mg minerals, such as olivine, clinopyroxene, and orthopyroxene in the dacites (Kiss et al., 2014; Vinkler et al., 2007) suggests that mafic magma also played an important role in the magma evolution. Harangi, Novák, et al. (2015) detected a lower crustal low resistivity anomaly, which might represent the mafic magma accumulation. Thus, we propose that most of the CO_2 gases could come directly from the presumed mafic-magma accumulation zone at the lower crust through fractures (Kis et al., 2017), whereas only limited amount of gases is derived from the mushy magma storage.

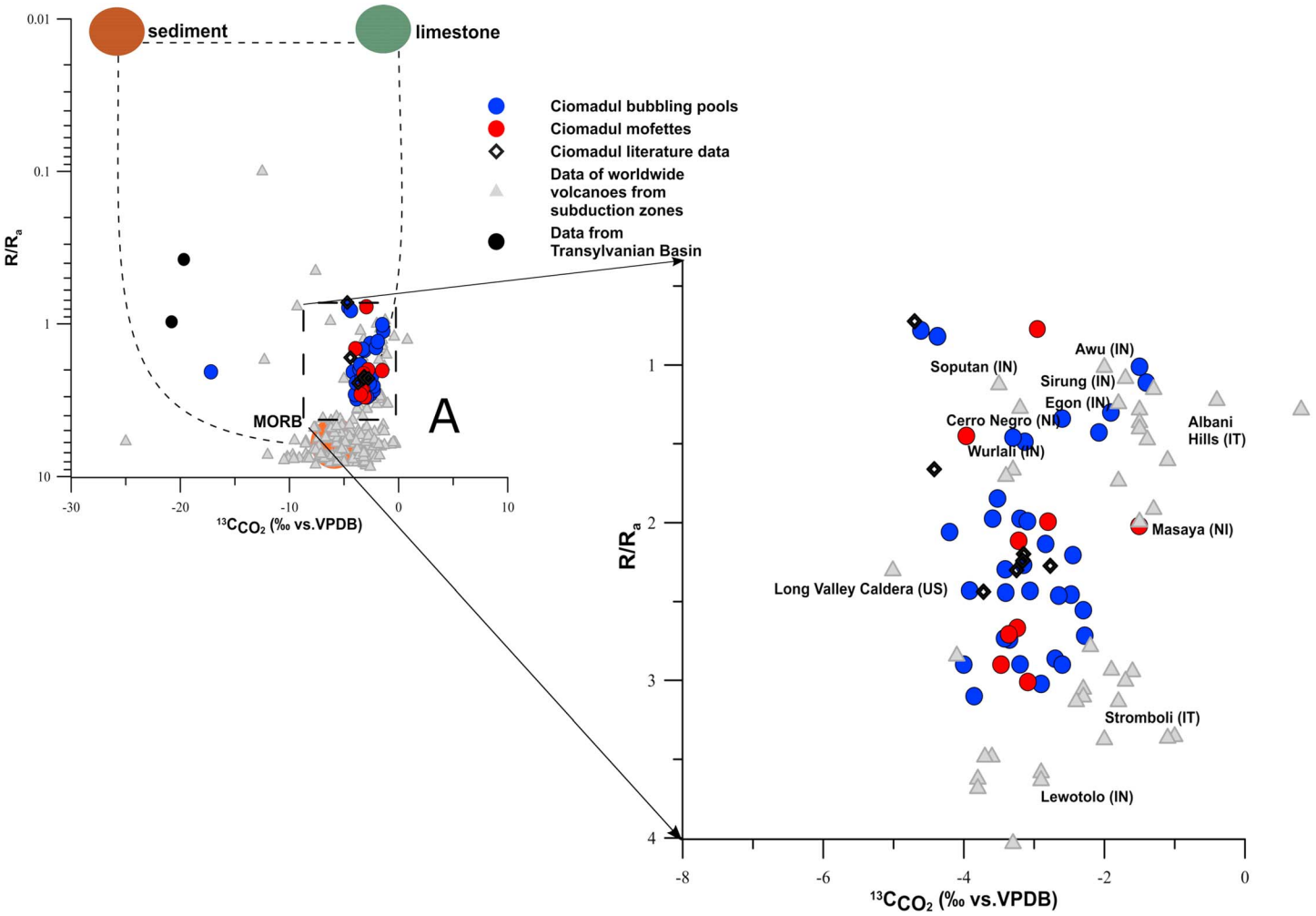

Figure 8. (a, b) Correlation diagram (Ciotoli et al., 2013) plotting He isotopic ratios (R/R_a) versus $^{13}C_{CO2}$ (VPDB) of Ciomadul gas emissions. Lines show the theoretical mixing between a mantle end member (MORB) and a crustal end member represented by marine limestone and organic sediment carbon (Sano & Marty, 1995, Sherwood-Lollar et al., 1997). Literature data for comparison: data after Althaus et al. (2000), Vaselli et al. (2002), Baciu et al. (2007, 2017), Frunzeti et al. (2013). Data on individual volcanoes worldwide are based on the compilation of Mason et al. (2017) from the data presented by Allard (1983), Marty and Giggenbach (1990), Poorter et al. (1991), Varekamp et al. (1992), Sturchio et al. (1993), Sano et al. (1994), Sano and Marty (1995), Tedesco et al. (1995), Hilton (1996), Sano and Williams (1996), Allard et al. (1997), Fischer et al. (1998), van Soest et al. (1998), Pedroni et al. (1999), Lewicki et al. (2000), Parello et al. (2000), Favara et al. (2001), Snyder et al. (2001), Shaw et al. (2003), Symonds et al. (2003), Jaffe et al. (2004), Capasso et al. (2005), Carapezza et al. (2007), de Leeuw et al. (2007), Werner et al. (2009), Capaccioni et al. (2011), Tassi et al. (2011), Aguilera et al. (2012), Melián et al. (2012), and Caracausi et al., 2013.

Vaselli et al. (2002) already suggested that the emitted gases in Southern Harghita could have a magmatic component. Based on our new measurements, we support this interpretation, particularly in the area of Ciomadul volcano. Assuming that a deep-seated mafic magma body can be the main source of the CO_2 gases and considering that it is characterized by relatively low $^3He/^4He$ isotope signature (3.1 R_a) inherited by the mantle source region, we can use this value to calculate the relative magmatic component of the emitted gases (Sano & Wakita, 1985). If no interaction with crustal fluids occurred, the magmatic component in the gases could exceed even the 80%. Remarkably, we obtained such high values for the areas having a larger diffusive CO_2 flux. This high magmatic He content of the gases is not unique and resembles what Trasatti et al. (2018) proposed for Colli Albani volcanic complex, another long-dormant volcanic field, where they assumed more than 80% mantle-derived component in the emitted CO_2 gases. However, the magmatic component can be lower, if interaction between the ascending gases with crustal gases occurred at shallow crustal depth, a possibility what we cannot test at this stage but requires further studies.

6. Conclusions

We investigated 31 gas emissions at the Ciomadul volcano, a long-dormant PAMS volcano in Eastern-Central Europe, to constrain the origin of the emitted volatiles and the possible processes that modify their chemistry during the transfer of these fluids toward the surface. The carbon and helium isotopic compositions provide evidence for a significant magmatic component. Our study shows a clear magmatic component in the emitted fluids and the highest values correspond to the area characterized by the highest CO_2 flux from soil, so the high fluxes can be associated with the highest contribution of volatiles derived from a magma body.

The relatively large CO_2 gas emission and significant magmatic component of the gases are consistent with geophysical and petrologic models (Harangi, Lukács, et al., 2015; Harangi, Novák, et al., 2015; Popa et al., 2012), that a degassing magmatic intrusion could still exist beneath Ciomadul. A long-standing silicic crystal mush body should be developed in the shallow crust, while a mafic magma accumulation zone is inferred at the lower crustal level. The magmatic gases could be derived either from a deep mafic magma and/or from the volatile accumulation zones developed in the shallow crustal felsic-crystal mush body. Petrology and geochemistry of the erupted dacitic magma imply that upper crustal contamination played no or subordinate role and the primary magmas could have derived from a mantle source contaminated by subduction-related fluids that is consistent with the He and C isotope composition of the gases emitted at Ciomadul volcano. Thus, a magma source with relatively low He isotope value (3.10 R_a), similar to what was proposed for volcanic systems in central Italy seems to be viable beneath Ciomadul. This differs from the SCLM value detected at the nearby Persani volcanic field (Althaust et al., 1998; this study) and also in the Pannonian basin (Bräuer et al., 2016; Cornides, 1993; Palcsu et al., 2014) and requires a spatially variable modified lithospheric mantle even a small scale. The isotopic composition (He and CO_2) of the emitted volatiles implies interaction of crustal gases to varying degrees, although some of them could reach the surface without major modification.

Acknowledgments
Information regarding the support of the conclusions of this work can be found in the tables and within the text. This research on the Ciomadul volcano was initiated during the MTA Postdoctoral Fellowship of Boglárka-Mercedesz Kis and belongs to the scientific project supported by the OTKA (Hungarian National Research Fund) K116528. The research was also supported by the European Union and the State of Hungary, cofinanced by the European Regional Development Fund in the project of GINOP-2.3.2-15-2016-00009 "ICER," and we acknowledge the support of the Deep Energy Community and Reservoirs and Fluxes Community of the Deep Carbon Observatory. Thorough reviews and constructive comments provided by Emilie Roulleau and Daniele Pinti helped considerably to clarify the ideas described in the paper. We thank Timothy Jull who provided a final polishing of the English of the manuscript.

References

Aguilera, F., Tassi, F., Darrah, T., Moune, S., & Vaselli, O. (2012). Geochemical model of magmatic-hydrothermal system at the Lastarria volcano, Northern Chile. *Bulletin of Volcanology*, *74*(1), 119–134. https://doi.org/10.1007/s00445-011-0489-5

Agusto, M., Tassi, F., Caselli, A. T., Vaselli, O., Rouwet, D., Capaccioni, B., et al. (2013). Gas geochemistry of the magmatic-hydrothermal fluid reservoir in the Copahue-Cavihue Volcanic Complex (Argentina). *Journal of Volcanology and Geothermal Research*, *257*, 44–56. https://doi.org/10.1016/j.jvolgeores.2013.03.003

Aiuppa, A., Moretti, R., Federico, C., Giudice, G., Gurrieri, S., Liuzzo, M., et al. (2007). Forecasting Etna eruptions by real-time observation of volcanic gas composition. *Geology*, *35*(12), 1115–1118. https://doi.org/10.1130/G24149A.1

Allard, P. (1983). The origin of hydrogen, carbon, suplhur, nitrogen and rare gases in volcanic exhalations: Evidence from isotope geochemisty. In H. Tazieff, & J. C. Sabroux (Eds.), *Forecasting Volcanic Events*, (pp. 337–386). Elsevier: Amsterdam.

Allard, P., Carbonelle, J., Dajlevic, D., Le Bronec, J., Morel, P., Robe, M. C., et al. (1991). Eruptive and diffuse emissions of CO_2 from Mount Etna. *Nature*, *351*(6325), 387–391. https://doi.org/10.1038/351387a0

Allard, P., Jean-Baptiste, P., D'Alessandro, W., Parello, F., Parisi, B., & Flehoc, C. (1997). Mantle-derived helium and carbon in groundwaters and gases of Mount Etna, Italy. *Earth and Planetary Science Letters*, *148*(3-4), 501–516. https://doi.org/10.1016/S0012-821X(97)00052-6

Althaus, T., Niedermann, S., & Erzinger, J. (2000). Noble gas studies of fluids and gas exhalations in the East Carpathians, Romania. *Chemie der Erde*, *60*, 189–207.

Althaust, A., Niedermann, S., & Erzinger, J. (1998). Noble gas in ultramafic mantle xenoliths in the Persani Mountains, Transylvanian Basin, Romania. *Mineralogical Magazine*, *62A*(1), 43–44. https://doi.org/10.1180/minmag.1998.62A.1.23

Baciu, C., Caracausi, A., Etiope, G., & Italiano, F. (2007). Mud volcanoes and methane seeps in Romania: Main features and flux. *Annals of Geophysics*, *50*, 4. https://doi.org/10.4401/ag-4435

Baciu, C., Ionescu, A., & Etiope, G. (2017). Hydrocarbon seeps in Romania: Gas origin and release to the atmosphere. *Marine and Petroleum Geology*, *89*(1), 130–143. https://doi.org/10.1016/j.marpetgeo.2017.06.015

Bănciă, I. (1958). *Geology of the Eastern Carpathians*. Editura Stiintifica: Bucharest.

Barry, P. H., Hilton, D. R., Fischer, T. P., de Moor, J. M., Mangasini, F., & Ramirez, C. (2013). Helium and carbon isotope systematic of cold "mazucu" CO_2 vents and hydrothermal gases and fluid from Rungwe Volcanic Province, southern Tanzania. *Chemical Geology*, *339*, 141–156. https://doi.org/10.1016/j.chemgeo.2012.07.003

Barry, P. H., Hilton, D. R., Füri, E., Halldórsson, S. A., & Grönvold, K. (2014). Carbon isotope and abundance systematics of Icelandic geothermal gases, fluids and subglatial basalts with implications from mantle plume-related CO_2 fluxes. *Geochimica et Cosmochimica Acta*, *134*, 74–99. https://doi.org/10.1016/j.gca.2014.02.038

Berszán, J., Cs, J., Jánosi, K., Kristály, F., Péter, É., Szakáll, S., & Ütő, G. (2009). *The mineral waters of Szeklerland*. Tipographic: Miercurea Ciuc. (In Hungarian)

Bräuer, K., Geissler, W. H., Kämpf, H., Niedermann, S., & Rman, N. (2016). Helium and carbon isotope signatures of gas exhalations in the westernmost part of the Pannonian Basin (SE Austria/NE Slovenia): Evidence for active litospheric mantle degassing. *Chemical Geology*, *422*, 60–70. https://doi.org/10.1016/j.chemgeo.2015.12.016

Bräuer, K., Kämpf, H., Niedermann, S., & Strauch, G. (2018). Monitoring of helium and carbon isotopes in the western Eger Rift area (Czech Republic): Relationships with the 2014 seismic activity and indications for recent (2000-2016) magmatic unrest. *Chemical Geology*, *482*, 131–145. https://doi.org/10.1016/j.chemgeo.2018.02.017

Bräuer, K., Kämpf, H., Niedermann, S., Strauch, G., & Tesar, J. (2008). Natural laboratory NW Bohemia: Comprehensive fluid studies between 1992 and 2005 used to trace geodynamic processes. *Geochemistry, Geophysics, Geosystems*, *9*, Q04018. https://doi.org/10.1029/2007GC001921

Burton, M. R., Sawyer, G. M., & Granieri, D. (2013). Deep carbon emissions from volcanoes. *Reviews in Mineralogy and Geochemistry*, *75*(1), 323–354. https://doi.org/10.2138/rmg.2013.75.11

Caliro, S., Viveiros, F., Chiodini, G., & Ferreira, T. (2015). Gas geochemistry of hydrothermal fluids of the S. Miguel and Terceira Islands, Azores. *Geochimica et Cosmochimica Acta*, *168*, 43–57. https://doi.org/10.1016/j.gca.2015.07.009

Capaccioni, B., Aguilera, F., Tassi, F., Darrah, T., Poreda, R., & Vaselli, O. (2011). Geochemical and isotopic evidences of magmatic inputs in the hydrothermal reservoirs feeding the fumarolic discharges on Tacora volcano (Northern Chile). *Journal of Volcanology and Geothermal Research*, *208*(3-4), 77–85. https://doi.org/10.1016/j.jvolgeores.2011.09.015

Capasso, G., Carapezza, M., Federico, C., Inguaggiato, S., & Rizzo, A. (2005). Geochemical monitoring of the helium isotopic composition of fumarole gases and thermal waters. *Bulletin of Volcanology*, *68*(2), 118–134. https://doi.org/10.1007/s00445-005-0427-5

Capasso, G., Favara, R., Grassa, F., Inguaggiato, S., & Longo, M. (2005). On-line technique for preparation and measuring stable carbon isotope of total dissolved inorganic carbon in water samples ($\delta^{13}C_{TDIC}$). *Annals of Geophysics*, *48*(1), 159–166.

Caracausi, A., Favara, R., Giammanco, S., Italiano, F., Paonita, A., Pecoraino, G., & Rizzo, A. (2003). Mount Etna: Geochemical signals of magma ascentand unusually extensive plumbing system. *Geophysical Research Letters*, *30*(2), 1057. https://doi.org/10.1029/2002GL015463

Caracausi, A., Martelli, M., Nuccio, P. M., Paternoster, M., & Stuart, F. M. (2013). Active degassing of mantle-derived fluid: A geochemical study along the Vulture line, southern Apenninnes (Italy). *Journal of Volcanology and Geothermal Research*, *253*, 65–74. https://doi.org/10.1016/j.jvolgeores.2012.12.005

Caracausi, A., Nuccio, P. M., Favara, R., Nicolosi, M., & Paternoster, M. (2009). Gas hazard assessment at the Monticchio crater lakes of Mt. Vulture, a volcano in southern Italy. *Terra Nova*, *21*, 83–87. https://doi.org/10.11111/1365-3121.200800858

Caracausi, A., Paternoster, M., & Nuccio, P. M. (2015). Mantle CO_2 degassing at Mt. Vulture volcano (Italy): Relationship between CO_2 outgassing of volcanoes and the time of their last eruption. *Earth and Planetary Science Letters*, *411*, 268–280. https://doi.org/10.1016/j.epsl.2014.11.049

Carapezza, M. L., Badalamenti, B., Cavarra, L., & Scalzo, A. (2003). Gas hazard assessment in a densely inhabited area of Colli Albani Volcano (Cava dei Selci, Roma). *Journal of Volcanology and Geothermal Research*, *123*(1-2), 81–94. https://doi.org/10.1016/S0377-0273(03)00029-5

Carapezza, M. L., Barbieri, F., Ranaldi, M., Ricci, T., Tarchini, L., Barrancos, J., et al. (2012). Hazardous gas emissions from the flanks of the quiescent Colli Albani volcano (Rome, Italy). *Applied Geochemistry*, *27*(9), 1767–1782. https://doi.org/10.1016/j.apgeochem.2012.02.012

Carapezza, M. L., & Tarchini, L. (2007). Accidental gas emission from shallow pressurized aquifers at Alban Hills volcano (Rome, Italy): Geochemical evidence of magmatic degassing? *Journal of Volcanology and Geothermal Research*, *165*(1-2), 5–16. https://doi.org/10.1016/j.jvolgeores.2007.04.008

Cardellini, C., Chiodini, G., Frondini, F., Avino, R., Bagnato, E., Caliro, S., et al. (2017). Monitoring diffuse volcanic degassing during volcanic inrest: The case of Campi Flegrei (Italy). *Scientific Reports*, *7*(1), 6757. https://doi.org/10.1038/s41598-017-06941-2

Cashman, K. V., Sparks, S., & Blundy, J. D. (2017). Vertically extensive and unstable magmatic systems: An unified view of igneous processes. *Science*, *355*, 6331. https://doi.org/10.1126/eaay3055

Chiodini, G., Cardellini, C., Amato, A., Boschi, E., Caliro, S., Frondini, F., & Ventura, G.(2004). Carbon dioxide earth degassing and seismogenesis in central and southern Italy. *Geophysical Research Letters*, *31*, L07615. https://doi.org/10.1029/2004gl019480

Christopher, T., Edmonds, M., Humphreys, M. C. S., & Herd, R. A. (2010). Volcanic gas emissions from Soufriere Hills Volcano, Montserrat 1995-2009, with implications for mafic magma supply and degassing. *Geophysical Research Letters*, *37*, L00E04. https://doi.org/10.1029/2009GL041325

Christopher, T. E., Blundy, J., Cashman, K., Cole, P., Edmonds, M., Smith, P. J., et al. (2015). Crustal-scale degassing due to magma system destabilization and magma-gas decoupling at Soufriere Hills Volcano, Montserrat. *Geohemistry, Geophysics, Geosystems*, *16*, 2797–2811. https://doi.org/10.1002/2015GC005791

Ciotoli, G., Etiope, G., Florindo, F., Marra, F., Ruggiero, L., & Sauer, P. E. (2013). Sudden deep gas eruption nearby Rome's airport of Fiumicino. *Geophysical Research Letters*, *40*, 5632–5636. https://doi.org/10.1002/2013GL058132

Cloetingh, S. A. P. L., Burov, E., Matenco, L., Toussaint, G., Bertotti, G., Andriessen, P. A. M., et al. (2004). Thermo-mechanical controls on the mode of continental collision in the SE Carpathians (Romania). *Earth and Planetary Science Letters.*, *218*(1–2), 57–76. https://doi.org/10.1016/S0012-821X(03)00645-9

Comeau, J. M., Unsworth, M. J., & Cordell, D. (2016). New constraints on the magma distribution and composition beneath Volcan Uturuncu and the southern Bolivian Altiplano from magnetotelluric data. *Geosphere*, *12*(5), 1391–1421. https://doi.org/10.1130/GES01277.1

Comeau, M. J., Unsworth, M. J., Ticona, F., & Sunagua, M. (2015). Magnetotelluric images of magma distribution beneath Volcano Uturuncu, Bolivia: Implications for magma dynamics. *Geology*, *43*(3), 243–246. https://doi.org/10.1130/G36258.1

Condomines, M., Gronvold, K., Hooker, P. J., Muehlenbachs, K., O'Nions, R. K., Oskarsson, N., & Oxburgh, E. R. (1983). Helium, oxygen, strontium and neodymium isotopic relationships in Iceland volcanics. *Earth and Planetary Science Letters*, *66*, 125–136. https://doi.org/10.1016/0012-821X(83)90131-0

Cornides, I. (1993). Magmatic carbon dioxide at the crust's surface in the Carpathian Basin. *Geochemical Journal*, *27*(4/5), 241–249. https://doi.org/10.2343/geochemj.27.241

Correale, A., Martelli, M., Paonita, A., Rizzo, A., Brusca, L., & Scribano, V. (2012). New evidence of mantle heterogeneity beneath the Hyblean Plateau (southeast Sicily, Italy) as inferred from noble gases and geochemistry of ultramafic xenoliths. *Lithos*, *132-133*, 70–81. https://doi.org/10.1016/j.lithos.2011.11.007

Csontos, L., Nagymarosy, A., Horváth, D., & Kovác, M. (1992). Tertiary evolution of the intra Carpathian area: A model. *Tectonophysics*, *208*(1-3), 221–241. https://doi.org/10.1016/0040-1951(92)90346-8

de Leeuw, G., Hilton, D., Fischer, T. P., & Walker, J. (2007). The He-CO_2 isotope and relative abundance characteristics of geothermal fluids in El Salvador and Honduras: New constraints on volatile mass balance of the Central American Volcanic Arc. *Earth and Planetary Science Letters*, *258*(1-2), 132–146. https://doi.org/10.1016/j.epsl.2007.03.028

Demetrescu, C., & Andreescu, M. (1994). On the thermal regime of some tectonic units in a continental collision environment in Romania. *Tectonophysics*, *230*(3-4), 265–276. https://doi.org/10.1016/0040-1951(94)90140-6

Downes, H., Seghedi, I., Szakács, A., Dobosi, G., James, D. E., Vaselli, O., et al. (1995). Petrology and geochemistry of late Tertiary/Quaternarymafic alkaline volcanism in Romania. *Lithos*, *35*(1-2), 65–81. https://doi.org/10.1016/0024-4937(95)91152-Y

Edmonds, M. (2008). New geochemical insights into volcanic degassing. *Philosophical Transactions of the Royal Society A*, *366*, 4559–4579. https://doi.org/10.1098/stra.2008.0185

Falus, G., Tommasi, A., Ingrin, J., & Cs, S. (2008). Deformation and seismic anisotropy of the lithospheric mantle in the southeastern Carpathians inferred from the study of mantle xenoliths. *Earth and Planetary Science Letters*, *272*(1-2), 50–64. https://doi.org/10.1016/j.epsl.2008.04.035

Farrar, C. D., Sorey, M. L., Evans, W. C., Howle, J. F., Kerr, B. D., Kennedy, B. M., et al. (1995). Forest-killing diffuse CO_2 emission at Mammoth Mountain as a sign of magmatic unrest. *Nature*, *376*(6542), 675–678. https://doi.org/10.1038/376675a0

Favara, R., Giammanco, S., Inguaggiato, S., & Pecoraino, G. (2001). Preliminary estimate of CO_2 output from Pantelleria Island volcano (Sicily, Italy): Evidence for active mantle degassing. *Applied Geochemistry*, *16*(7-8), 883–894. https://doi.org/10.1016/S0883-2927(00)00055-X

Fischer, T., Horalek, J., Hrubcova, P., Vavrycuk, V., Bräuer, K., & Kämpf, H. (2014). Intra-continental earthquake swarms in West-Bohemia and Vogtland: A review. *Tectonophysics*, *611*, 1–27. https://doi.org/10.1016/j.tecto.2013.11.001

Fischer, T. P. (2008). Fluxes of volatiles (H_2O, CO_2, N_2, Cl, F) from arc volcanoes. *Geochemical Journal*, *42*(1), 21–38. https://doi.org/10.2343/geochemj.42.21

Fischer, T. P., Giggenbach, W. F., Sano, Y., & Williams, S. N. (1998). Fluxes and sources of volatiles discharged from Kudryavy, a subduction zone volcano, Kurile Islands. *Earth and Planetary Science Letters*, *160*(1-2), 81–96. https://doi.org/10.1016/S0012-821X(98)00086-7

Frunzeti, N. (2013). *Geogenic emissions of greenhouse gases in the Southern part of the Eastern Carpathians, (Doctoral dissertation)*, Retrieved from Faculty of Environmental Science and Engineering. Cluj-Napoca: Babes-Bolyai University. (In Romanian)

Gautheron, C., & Moreira, M. (2002). Helium signature of the subcontinental lithospheric mantle. *Earth and Planetary Science Letters*, *199*(1-2), 39–47. https://doi.org/10.1016/S0012-821X(02)00563-0

Grasu, C., Catana, C., & Bobos, I. (1996). *Petrology of the flysch formations in the inner Carpathians*. Editura Tehnica: Bucharest.

Harangi, S., Sági, T., Seghedi, I., & Ntaflos, T. (2013). Origin of basaltic magmas of Perşani volcanic field, Romania: A combined whole rock and mineral scale investigation. *Lithos*, *180-181*, 43–57. https://doi.org/10.1016/j.lithos.2013.08.025

Harangi, S., Lukács, R., Schmitt, A. K., Dunkl, I., Molnár, K., Kiss, B., et al. (2015). Constraints on the timing of Quaternary volcanism and duration of magma residence at Ciomadul volcano, east-central Europe, from combined U-Th/He and U-Th zircon geochronology. *Journal of Volcanology and Geothermal Research*, *301*, 66–80. https://doi.org/10.1016/j.jvolgeores.2015.05.002

Harangi, S., Molnár, M., Vinkler, A. P., Kiss, B., Jull, A. J. T., & Leonard, A. E. (2010). Radiocarbon dating of the last volcanic eruptions of Ciomadul volcano, Southeast Carpathians, eastern-central Europe. *Radiocarbon*, *52*(3), 1498–1507. https://doi.org/10.1017/S0033822200046580

Harangi, S., Novák, A., Kiss, B., Seghedi, I., Lukács, R., Szarka, L., et al. (2015). Combined magnetotelluric and petrologic constrains for the nature of the magma storage system beneath the Late Pleistocene Ciomadul volcano (SE Carpathians). *Journal of Volcanology and Geothermal Research*, *290*, 82–96. https://doi.org/10.1016/j.jvolgeores.2014.12.006

Hilton, D. (1996). The helium and carbon isotope systematics of a continental geothermal system: Results from monitoring studies at Long Valley caldera (California, U.S.A.). *Chemical Geology*, *127*(4), 269–295. https://doi.org/10.1016/0009-2541(95)00134-4

Hilton, D. R., Fischer, T. P., & Marty, B. (2002). Noble gases and volatile recycling at subduction zones. *Review in Mineralogy and Geochemistry*, *47*(1), 319–370. https://doi.org/10.2138/rmg.2002.47.9

Hilton, D. R., Hoogewerff, J. A., Van Bergen, M. J., & Hammerschmidt, K. (1992). Mapping magma sources in the east Sunda-Banda arcs, Indonesia: Constraints from helium isotopes. *Geochimica et Cosmochimica Acta*, *56*(2), 851–859. https://doi.org/10.1016/0016-7037(92)90105-R

Holland, G., & Gilfillan, S. (2013). Application of the noble gases to the variability of CO2 storage. In P. Burnad (Ed.), *The noble gases as geochemical tracers*, (pp. 177–223). Springer, Berlin-Heidelberg.

Horváth, F., Bada, G., Windhoffer, G., Csontos, L., Dombradi, E., Dövényi, P., et al. (2006). The geodynamic atlas of the Pannonian Basin: Euro-conform maps and explanations. *Magyar Geofizika*, *47*(4), 133–137. (In Hungarian)

Ianovici, V., & Rădulescu, D. (1968). *Geological map 1:200000 L-35-XIV, 20th Sheet-Odorhei*. Bucharest: Geological Institute of Romania. (In Romanian)

Ismail-Zadeh, A., Matenco, L., Radulian, M., Cloetingh, S., & Panza, S. (2012). Geodynamics and intermediate-depth seismicity in Vrancea (the south-eastern Carpathians): Current state-of-the art. *Tectonophysics*, *530-531*, 50–79. https://doi.org/10.1016/j.tecto.2012.01.016

Italiano, F., Kis, B. M., Baciu, C., Ionescu, A., Harangi, S., & Palcsu, L. (2017). Geochemistry of dissolved gases from the Eastern Carpathians-Transylvanian Basin boundary. *Chemical Geology*, *469*, 117–128. https://doi.org/10.1016/j.chemgeo.2016.12.019

Jaffe, L. A., Hilton, D. R., Fischer, T. P., & Hartono, U. (2004). Tracing magma sources in an arc-arc collision zone: Helium and carbon isotope and relative abundance systematics of theSanhihe Arc, Indonesia. *Geochemistry, Geophysics, Geosystems*, *5*, Q04J10. https://doi.org/10.1029/2003GC000660

Jánosi, C. (1980). *The hydrogeology of the inferior part of the Ciuc Basin, with focus on the mineral water springs*. (Doctoral dissertation). Retrieved from Faculty of Biology and Geology. Cluj-Napoca: Babes-Bolyai University. (In Romanian)

Jánosi Cs., Berszán J. & Péter É. (2011). The mineral baths of Ciomadul Mountains, Acta Siculica 2011, Miercurea Ciuc, (pp.41-56) In Hungarian.

Karátson, D., & Timár, G. (2005). Comparative volumetric calculations of two segments of the Carpathian Neogene/Quaternary volcanic chain using SRTM elevation data: Implications for erosion and magma output rates. *Zeitschrift fur Geomorphologie*, *140*, 19–35. Supplementary Issues

Karátson, D., Wulf, S., Veres, D., Magyari, E., Gertisser, R., Timár-Gabor, A., et al. (2016). The latest explosive eruptions of Ciomadul (Csomád) volcano, East Carpathians—A tephrostratigrapic approach for the 51-29 ka BP time interval. *Journal of Volcanology and Geothermal Research*, *319*, 29–51. https://doi.org/10.1016/j.jvolgeores.2016.03.005

Kato, A., Terakawa, T., Yamanaka, Y., Maeda, Y., Horikawa, S., Matsushiro, K., & Okuda, T. (2015). Preparatory and precursory processes leading up to the 2014 phreatic eruption of Mount Ontake. Japan. *Earth, Planets and Space*, *67*(1), 111. https://doi.org/10.1186/s40623-015-0288-x

Kennedy, B. M., & van Soest, M. C. (2006). A helium isotope perspective on the Dixie Valley, Nevada, hydrothermal system. *Geothermics*, *35*(1), 26–43. https://doi.org/10.1016/j.geothermics.2005.09.004

Kis, B. M., Ionescu, A., Cardellini, C., Harangi, S., Baciu, C., Caracausi, C., & Viveiros, F. (2017). Quantification of carbon dioxide emissions of Ciomadul, the youngest volcano of the Carpathian-Pannonian Region (Eastern-Central Europe, Romania). *Journal of Volcanology and Geothermal Research*, *341*, 119–130. https://doi.org/10.1016/j.jvolgeores.2017.05.025

Kiss, B., Harangi, S., Ntaflos, T., Mason, P., & Pál-Molnár, E. (2014). Amphibole perspective to unravel pre-eruptive processes and conditions in volcanic plumbing systems beneath intermediate arc volcanoes: A case study from Ciomadul volcano (SE Carpathians). *Contributions to Mineralogy and Petrology*, *167*(3). https://doi.org/10.1007/s00410-014-0986-6

Konstantinou, K. I., Lin, C.-H., & Liang, W.-T. (2007). Seismicity characteristics of a potentially active Quaternary volcano: The Tatun Volcano Group, northern Taiwan. *Journal of Volcanology and Geothermal Research*, *160*(3-4), 300–318. https://doi.org/10.1016/j.volgeores.2006.09.009

Lee, H., Muirhead, J., Fischer, T. P., Ebinger, C. J., Kattenhorn, S. A., Sharp, Z. D., & Kianji, G. (2016). Massive and prolonged deep carbon emissions associated with continental rifting. *Nature Geoscience*, *9*(2), 145–149. https://doi.org/10.1038/ngeo2622

Lewicki, J. L., Fischer, T., & Williams, S. N. (2000). Chemical and isotopic compositions of fluid at Cumbal Volcani, Colombia: Evidence for magmatic contribution. *Bulletin of Volcanology*, *62*(4-5), 347–361. https://doi.org/10.1007/s004450000100

Lin, C. H., & Pu, H. C. (2016). Very-long-period seismic signals at the Tatun Volcano Group, northern Taiwan. *Journal of Volcanology and Geothermal Research*, *328*, 230–236. https://doi.org/10.1016/j.volgeores.2016.11.007

Liotta, M., & Martelli, M. (2012). Dissolved gases in brackish thermal waters: An improved analytical method. *Geofluids*, *12*(3), 236–244. https://doi.org/10.1111/j.1468-8123.2012.00365.x

Lukács, R., Guillong, M., Schmitt, A. K., Molnár, K., Bachman, O., & Harangi, S. (2018). La-ICP-MS and SIMS U-Pb and U-Th zircon geochronological data of Late Pleistocene lava domes of the Ciomadul Volcanic Dome Complex (Eastern Carpathians). *Data in Brief*, *18*, 808–813. https://doi.org/10.1016/j.dib.2018.03.100

Mandarano, M., Paonita, A., Martelli, M., Viccaro, M., Nicotra, E., & Millar, I. L. (2016). Revealing magma degassing below closed-conduit active volcanoes: Geochemical features of volcanic rocks versus fumarolic fluids at Vulcano (Aeolian Islands, Italy). *Lithos*, *248-251*, 272–287. https://doi.org/10.1016/j.lithos.2016.01.026

Martelli, M., Nuccio, P. M., Stuart, F. M., Burgessd, R., Ellamc, R. M., & Italiano, F. (2004). Helium–strontium isotope constraints on mantle evolution beneath the Roman Comagmatic Province, Italy. *Earth and Planetary Science Letters*, *224*(3-4), 295–308. https://doi.org/10.1016/j.epsl.2004.05.025

Marty, B., & Giggenbach, W. F. (1990). Major and rare gases at White Island volcano, New Zealand: Origin and flux of volatiles. *Geophysical Research Letters*, *17*(3), 247–250. https://doi.org/10.1029/GL017i003p00247

Marty, B., & Jambon, A. (1987). C/3He in volatile fluxes from the solid Earth: Implications for carbon geodynamics. *Earth and Planetary Science Letters*, *83*(1-4), 16–26. https://doi.org/10.1016/0012-821X(87)90047-1

Mason, E., Edmonds, M., & Turchyn, A. (2017). Remobilization of crustal carbon may dominate volcanic arc emissions. *Science*, *357*, 290–294. https://doi.org/10.1126/science.aan5049

Mason, P., Downes, H., Thirlwall, M.F., Seghedi, I., Szakács, A., Lowry, D., Mattey, D., (1996). Crustal assimilation as a major petrogenetic process in the East Carpathian Neogene and Quaternary Continental Margin Arc, Romania

Mațenco, L., & Bertotti, G. (2000). Tertiary tectonic evolution of the external East Carpthians (Romania). *Tectonophysics*, *316*(3-4), 255–286. https://doi.org/10.1016/S0040-1951(99)00261-9

Mațenco, L., Bertotti, G., Leever, K., Cloething, S., Schmidt, S. M., Tărăpoancă, M., & Dinu, C. (2007). Large-scale deformation in a locked collisional boundary: Interplay between subsidence and uplift, intraphase stress, and inherited litospheric structure in the large stage of the SE Carpathian evolution. *Tectonics*, *26*, TC4011. https://doi.org/10.1029/2006TC001951

Mazot, A., Rouwet, D., Taran, Y., Inguaggiato, S., & Varley, N. (2011). CO_2 and He degassing at El Chicón volcano, Chiapas, Mexico: Gas flux, origin and relationship with local and regional tectonics. *Bulletin of Volcanology*, *73*, 423–441. https://doi.org/10.1007/s00445-010-0443-y

Melián, G., Tassi, F., Pérez, N., Hernández, P., Sortino, F., Vaselli, O., et al. (2012). A magmatic source for fumaroles and diffuse degassing from the summit crater of Teide Volcano (Tenerife, Canary Islands): A geochemical evidence for the 2004-2005 seismic-volcanic crisis. *Bulletin of Volcanology*, *74*(6), 1465–1483. https://doi.org/10.1007/s00445-012-0613-1

Molnár, K., Harangi, S., Lukács, R., Dunkl, I., Schmitt, A. K., Kiss, B., et al. (2018). The onset of the volcanism in the Ciomadul Volcanic Dome Complex (Eastern Carpathians): Eruption chronology and magma type variation. *Journal of Volcanology and Geothermal Research*, *354*, 39–56. https://doi.org/10.1016/j.jvolgeores.2018.01.025

Molnár, K., Lukács, R., Dunkl, I., Schmitt, A. K., Kiss, B., Seghedi, I., et al. (2019). Episodes of dormancy and eruption of the Late Pleistocene Ciomadul volcanic complex (Eastern Carpathians, Romania) constrained by zircon geochronology. *Journal of Volcanology and Geothermal Research*, *373*, 133–147. https://doi.org/10.1016/j.jvolgeores.2019.01.025

Moriya, I., Okuno, M., Nakamura, E., Szakács, A., & Seghedi, I. (1995). Last eruption and its ^{14}C age of Ciomadul Volcano, Romania. *Summaries of Researches Using AMS at Nagoya University*, *6*, 82–91.

Moriya, I., Okuno, M., Nakamura, T., Ono, K., & Seghedi, I. (1996). Radiocarbon ages of charcoal fragments from the pumice flow deposits of the last eruption of Ciomadul Volcano, Romania. *Summaries of Researches Using AMS at Nagoya University*, *3*, 252–255.

Moussallam, Y., Bani, P., Schipper, C. I., Cardona, C., Franco, L., Barnie, T., et al. (2018). Unrest and the Nevados de Chillan volcanic complex: A failed or yet to unfold magmatic eruption. *Volcanica*, *1*(1), 19–32. https://doi.org/10.30909/vol.01.01.1932

Nicolaescu, V. (1973). Contributions to the knowledge on the Cretaceous flysch of the western part of Bodoc Mts. *Studii şi cercetări Geologie Geofizica,Geografie*, *18*(2), 479–488. (In Romanian)

O'Nions, R. K., & Oxburgh, E. R. (1988). Helium, volatile fluxes and the development of the continental crust. *Earth and Planetary Science Letters*, *90*(3), 331–347. https://doi.org/10.1016/0012-821X(88)90134-3

Oppenheimer, C., Fischer, T. P., & Scaillet, B. (2014). Volcanic degassing: Process and impact. In H. D. Holland, & K. K. Turekian (Eds.), *Treatise on Geochemistry*, (2nd ed.pp. 111–179). Oxford: Elsevier. https://doi.org/10.1016/B978-0-08-095975-7.00304-1

Ozima, M., & Podosek, F. A. (2002). *Noble gas geochemistry*. Cambridge: Cambridge University Press.

Palcsu, L., Vető, I., Futó, I., Vodila, G., Papp, L., & Major, Z. (2014). In-reservoir mixing of mantle-derived CO_2 and metasedimentary CH_4-N_2 fluids. Noble gas and stable isotope study of two multistached fields (Pannonian Basin System, W-Hungary). *Marine and Petroleum Geology*, *54*, 216–227. https://doi.org/10.1016/j.marpetgeo.2014.03.013

Panaiotu, C. G., Jicha, B. R., Singer, B. S., Tugui, A., Seghedi, I., Panaiotu, A. G., & Necula, C. (2013). $^{40}Ar/^{39}Ar$ chronology and paleomagnetism of Quaternary basaltic lavas from the Perşani Mountains (East Carpathians). *Physics of the Earth and Planetary Interiors*, *221*, 1–24. https://doi.org/10.1016/j.pepi.2013.06.007

Panaiotu, C. G., Pécskay, Z., Hambach, U., Seghedi, I., Panaiotu, C. E., Tetsumaru, I., et al. (2004). Short-lived Quaternary volcanism in the Persani Mountains (Romania) revealed by combined K–Ar and paleomagnetic data. *Geologica Carpathica*, *55*(4), 333–339.

Paonita, A., Caracausi, A., Iacono-Marziano, G., Martelli, M., & Rizzo, A. (2012). Geochemical evidence for mixing between fluids exsolved at different depths in the magmatic system of Mt. Etna (Italy). *Geochimica et Cosmochimica Acta*, *84*, 380–394. https://doi.org/10.1016/j.gca.2012.01.028

Paonita, A., Longo, M., Bellomo, S., D'Alessandro, W., & Brusca, L. (2016). Dissolved inert gases (He, Ne and N_2) as markers of groundwater flow and degassing areas at Mt. Etna volcano (Italy). *Chemical Geology*, *443*, 10–21. https://doi.org/10.1016/j.chemgeo.2016.09.018

Parello, F., Allard, P., D'Alessandro, W., Federico, C., Jean-Baptiste, P., & Catani, O. (2000). Isotope geochemistry of Pantelleria volcanic fluids, Sicily Channel rift: A mantle volatile end-member for volcanism in southern Europe. *Earth and Planetary Science Letters*, *180*(3–4), 325–339. https://doi.org/10.1016/S0012-821X(00)00183-7

Pécskay, Z., Lexa, J., Szakács, A., Seghedi, I., Balogh, K., Konecny, V., et al. (2006). Geochronology of Neogene magmatism in the Carpathian arc and intra-Carpathian area. *Geologica Carpathica*, *57*(6), 511–530.

Pedroni, A., Hammerschidt, K., & Friedrichsen, H. (1999). He, Ne, Ar and C isotope systematics of geothermal emanations in the Lesser Antilles Islands Arc. *Geochimicaet Cosmochimica Acta*, *63*(3-4), 515–532. https://doi.org/10.1016/S0016-7037(99)00018-6

Pik, R., & Marty, B. (2008). Helium isotopic signature of modern and fossil fluids associated with the Corinth rift fault zone (Greece): Implication for fault connectivity in the lower crust. *Chemical Geology*, *266*(1-2), 67–75. https://doi.org/10.1016/j.chemgeo.2008.09.024

Pizzino, L., Galli, G., Mancini, C., Quattrocchi, F., & Scarlato, P. (2002). Natural gas hazard (CO_2 and ^{222}Rn) within a quiescent volcanic region and its relations with tectonics: The case of Ciampino-Marino Area, Albani Hills Volcano, Italy. *Natural Hazards*, *27*(3), 257–287. https://doi.org/10.1023/A:1020398128649

Poorter, R., Varekamp, J., Poreda, R., Van Bergen, M., & Kreuen, R. (1991). Chemical and isotopic compositions of volcanic gases from the east Sunda and Banda arcs, Indonesia. *Geochimica et Cosmochimica Acta*, *55*(12), 3798–3807. https://doi.org/10.1016/0016-7073(91)90075-G

Popa, M., Radulian, M., Szakács, A., Seghedi, I., & Zaharia, B. (2012). New seismic and tomography data inthe southern part of the Harghita Mountains (Romania, Southeastern Carpathians): Connection with recent volcanic activity. *Pure Applied Geophysics*, *169*(9), 1557–1573. https://doi.org/10.1007/s00024-011-0428-6

Rădulescu, D., Peter, E., Stanciu, C., Stefanescu, M., & Veliciu, S. (1981). Discussion on the geothermal anomalies within South Harghita Mountains. *Studii si Cercetari Geologie, Geografie, Geofizica, Seria Geologie*, *26*(2), 169–184. In Romanian

Rizzo, A. L., Barbieri, F., Carapezza, M. L., Di Piazza, A., Francalanci, L., Sortino, F., & D'Alessandro, W. (2015). New mafic magma refilling a quiescent volcano: Evidence from He-Ne-Ar isotopes during the 2011–2012 unrest at Santorini, Greece. *Geochemistry, Geophysics, Geosystems*, *16*, 798–814. https://doi.org/10.1002/2014GC005653

Roulleau, E., Sano, Y., Takahata, N., Yang, F. T., & Takahashi, H. A. (2015). He, Ar, N and C isotope compositions in Tatun Volcanic Group (TVG), Taiwan: Evidence for an important contribution of pelagic carbonates in the magmatic source. *Journal of Volcanology and Geothermal Research*, *303*, 7–15. https://doi.org/10.1016/j.volgeores.2015.07.017

Roulleau, E., Tardani, D., Sano, Y., Takahata, N., Vinet, N., Bravo, F., et al. (2016). New insight from noble gas and stable isotopes of geothermal/hydrothermal fluids at Caviahue-Copahue Volcanic Complex: Boiling steam separation and water-rock interaction at shallow depth. *Journal of Volcanology and Geothermal Research*, *328*, 70–83. https://doi.org/10.1016/j.jvolgeores.2016.10.007

Rouwet, D., Hidalgo, S., Joseph, E. P., & González-Ilama, G. (2017). Fluid geochemistry and volcanic unrest: Dissolving the haze in time and space. In *Advances in Volcanology*, (pp. 221–239). Berlin, Heidelberg: Springer. https://doi.org/10.1007/11157_2017_12

Rouwet, D., Sandri, L., Marzocchi, W., Gottsmann, J., Selva, J., Tonini, R., & Papale, P. (2014). Recognizing and tracking volcanic hazards related to non-magmatic unrest: A review. *Journal of Applied Volcanology*, *3*(1), 1–17. https://doi.org/10.1186/s13617-014-0017-3

Royden, L. H., Horváth, F., & Burchfiel, B. C. (1982). Transform faulting, extension and subduction in the Carpathian Pannonian Region. *GSA Bulletin*, *93*(8), 717–725. https://doi.org/10.1130/0016-7606(1982)93

Rudnick, R. L., & Gao, S. (2003). Composition of the continental crust. *Treatise in Geochemistry*, *3*, 1–64. https://doi.org/10.1016/B0-08-043751-6/03016-4

Ruzié, L., Moreira, M., & Crispi, O. (2012). Noble gas isotopes in hydrothermal volcanic fluids of La Soufriére volcano, Guadeloupe, Lesser Antilles arc. *Chemical Geology*, *304-305*, 158–165. https://doi.org/10.1016/j.chemgeo.2012.02.012

Sano, Y., Hirabayashi, J.-I., Oba, T., & Gamo, T. (1994). Carbon and helium isotopic ratios at Kusatsu-Shirane volcano, Japan. *Applied Geochemistry*, *9*(4), 371–377. https://doi.org/10.1016/0883-29274)90059-0

Sano, Y., Kagoshima, T., Takahata, N., Nishio, Y., Roulleau, E., Pinti, D. L., & Fischer, T. P. (2015). Ten-year helium anomaly prior to the 2014 Mt. Ontake eruption. *Scientific Reports*, *5*(1), 13069. https://doi.org/10.1038/srep13069

Sano, Y., & Marty, B. (1995). Origin of carbon in fumarolic gas from island arcs. *Chemical Geology*, *119*(1-4), 265–274. https://doi.org/10.1016/0009-2541(94)00097-R

Sano, Y., & Wakita, H. (1985). Geographical distribution of $^3He/^4He$ ratios in Japan: Implications for arc tectonics and incipient magmatism. *Journal of Geophysical Research*, *90*(B10), 8729–8741. https://doi.org/10.1029/JB090iB10p08729F

Sano, Y., & Williams, S. N. (1996). Fluxes of mantle and subducted carbon along convergent plate boundaries. *Geophysical Research Letters*, *23*(20), 2749–2752. https://doi.org/10.1029/96GL02260

Sarbu, S., Aerts, J. W., Flot, J. F., Van Spanning, R. J. M., Baciu, C., Ionescu, A., et al. (2018). Sulfur Cave (Romania), an extreme environment with microbial mats in a CO_2-H_2S/O gas chemocline dominated by mycobacteria. *International Journal of Speleology*, *47*(2), 173–187. https://doi.org/10.5038/1827-806X.47.2.2164

Seghedi, I., Downes, H., Harangi, S., Mason, P. R. D., & Pécskay, Z. (2005). Geochemical response of magmas to Neogene–Quaternary continental collision in the Carpathian–Pannonian region: A review. *Tectonophysics*, *410*(1-4), 485–499. https://doi.org/10.1016/j.tecto.2004.09.015

Seghedi, I., Downes, H., Szakács, A., Mason, P. R. D., Thirlwall, M. F., Rosu, E., et al. (2004). Neogene-Quaternary magmatism and geodinamics in the Carpathian-Pannonian region: A synthesis. *Lithos*, *72*(3-4), 117–146. https://doi.org/10.1016/j.lithos.2003.08.006

Seghedi, I., Maţenco, L., Downes, H., Mason, P. R. D., Szakács, A., & Pécskay, Z. (2011). Tectonic significance of changes in post-subduction Pliocene-Quaternary magmatism in the south east part of the Carpathian-Pannonian Region. *Tectonophysics*, *502*(1-2), 146–157. https://doi.org/10.1016/j.tecto.2009.12.003

Seghedi, I., Popa, R. G., Panaiotu, C. G., Szakács, A., & Pécskay, Z. (2016). Short-lived eruptive episodes during the construction of a Na-alkalic basaltic field (Perşani Mountains, SE Transylvania, Romania). *Bulletin of Volcanology*, *78*(10), 69. https://doi.org/10.1007/s00445-016-1063-y

Seghedi, I., & Szakács, A. (1994). The Upper Pliocene–Pleistocene effusive and explosive basalticvolcanism from the Perşani Mountains. *Romanian Journal of Petrology*, *76*, 101–107.

Seghedi, I., Szakács, A., Udrescu, C., Stoian, M., & Graban, G. (1987). Trace element geochemistry of the South Harghita volcanic (East Carpathians). Calc-alkaline and shoshinitic associations. *Dari de Seama a Sedintelor Institutului Geologic si Geofizic*, *72*(73), 1.

Shaw, A. M., Hilton, D. R., Fischer, T. P., Walker, J. A., & Alvarado, G. E. (2003). Contrasting He-C relationships in Nicaragua and Costa Rica: Insights into C cycling through subduction zones. *Earth and Planetary Science Letters*, *214*(3-4), 499–513. https://doi.org/10.1016/S0012-821X(03)00401-1

Sherwood-Lollar, B., Ballentine, C. J., & Onions, R. K. (1997). The fate of mantle-derived carbon in a continental sedimentary basin: Intergration of C He relationships and isotope signatures. *Geochimica et Cosmochimica Acta*, *61*(11), 2295–2307. https://doi.org/10.1016/S0016-7037(97)00083-5

Snyder, G., Poreda, R., Hunt, A., & Fehn, U. (2001). Regional variations in volatile composition: Isotopic evidence for carbonate recycling in the Central American volcanic arc. *Geochemistry, Geophysics, Geosystems*, *2*(10), 1057. https://doi.org/10.1029/2001GC000163

Sorey, M. L., Evans, W. C., Kennedy, B. M., Farrar, C. D., Hainsworth, L. J., & Hausback, B. (1998). Carbon dioxide and helium emission from a reservoir of magmatic gas beneath Mammoth Mountain, California. *Journal of Geophysical Research*, *103*(B7), 15,303–15,323. https://doi.org/10.1029/98JB01389

Sparks, R. S. J., Folkes, C. B., Humphreys, M. C. S., Barfod, D. N., Clavero, J., Sunagua, M. C., et al. (2008). Uturuncu volcano, Bolivia: Volcanic unrest due to mid-crustal magma intrusion. *American Journal of Science*, *308*(6), 727–769. https://doi.org/10.2475/06.2008.01

Sparks, S., & Cashman, K. (2017). Dynamic magma systems: Implications for forecasting volcanic activity. *Elements*, *13*(1), 35–40. https://doi.org/10.2113/gselements.13.1.35

Sturchio, N. C., Williams, S. N., & Sano, Y. (1993). The hydrothermal system of Volcan Purace, Colombia. *Bulletin of Volcanology*, *55*(4), 289–296. https://doi.org/10.1007/BF00624356

Symonds, R.B., Poreda, R.J., Evans, W.C., Janik, C.J. & Ritchie, B.E. (2003). Mantle and crustal sources of carbon, nitrogen and noble gases in Cascade-Range and Aleutian-Arc volcanic gases.*US Geological Survey Open-File Report*, 03–436

Szakács, A., & Seghedi, I. (1987). Base surge deposits in the Ciomadul Massif (South Harghita Mountains). *Dari de Seama ale sedintelor Institutului Geologic Geofizic*, *74*(1), 175–180.

Szakács, A., & Seghedi, I. (1995). The Călimani-Gurghiu-Harghita volcanic chain, East Carpathians, Romania: Volcanological features. *Acta Volcanologica*, *7*, 145–153.

Szakács, A., & Seghedi, I. (2013). The relevance of volcanic hazard in Romania: Is there any? *Environmental Engineering and Management Journal*, *12*, 125–135. https://doi.org/10.30638/eemj.2013.015

Szakács, A., Seghedi, I., & Pécskay, Z. (1993). Pecularities of South Harghita Mts. as terminal segment of the Carpathian Neogene to Quaternary volcanic chain. *Revue Roumaine de Geophysique*, *37*, 21–36.

Szakács, A., Seghedi, I., Pécskay, Z., & Mirea, V. (2015). Eruptive history of a low-frequency and low-output rate Pleistocene volcano, Ciomadul, South Harghita Mts., Romania. *Bulletin of Volcanology*, *77*(2). https://doi.org/10.1007/s00445-014-0894-7

Tassi, F., Aguilera, F., Benavente, O., Paonita, A., Chiodini, G., Caliro, S., et al. (2016). Geochemistry of fluid discharges from Peteroa volcano (Argentina-Chile) in 2010-2015: Insights into compositional changes related to the fluid source region(s). *Chemical Geology*, *432*, 41–53. https://doi.org/10.1016/j.chemgeo.2016.04.007

Tassi, F., Aguilera, F., Darrah, T., Vaselli, O., Capaccioni, B., Poreda, R. J., & Delgado Huertas, A. (2010). Fluid geochemistry of hydrothermal systems in the Arica-Parinacota, Taracapa and Antofagasta regions (northern Chile). *Journal of Volcanology and Geothermal Research*, *192*(1-2), 1–15. https://doi.org/10.1016/j.jvolgeores.2010.02.006

Tassi, F., Aguilera, F., Vaselli, O., Darrah, T., & Medina, E. (2011). Gas discharges from four remote volcanoes in Chile (Putana, Olca, Irruputuncu and Alitar): A geochemical survey. *Annals of Geophysics*, *54*. https://doi.org/10.4401/ag-5173

Tassi, F., Nisi, B., Cardellini, C., Capecchiacci, F., Donnini, M., Vaselli, O., et al. (2013). Diffuse soil emission of hydrothermal gases (CO_2, CH_4, C_6H_6) at Solfatara crater (Campi Flegrei, Southern Italy). *Applied Geochemistry*, *35*, 142–153. https://doi.org/10.1016/j.apgeochem.2013.03.020

Tedesco, D., Miele, G., Sano, Y., & Tardani, J. P. (1995). Helium isotopic ratio in Vulcano island fumaroles: Temporal variations in shallow level mixing and deep magmatic supply. *Journal of Volcanology and Geothermal Research*, *64*(1-2), 117–128. https://doi.org/10.1016/0377-0273(94)00045-I

Torgersen, T., Drenkard, S., Stute, M., Schlosser, P., & Shapiro, A. (1995). Mantle helium in-ground waters of eastern North-America—Time and space constraints on sources. *Geology*, *23*(8), 675–678. https://doi.org/10.1130/0091-7613(1995)023<0675:MHIGWO>2.3.CO;2

Trasatti, E., Marra, F., Polcari, M., Etiope, G., Ciotoli, G., Darrah, T. H., et al. (2018). Coeval uplift and subsidence reveal magma recharging near Rome (Italy). *Geochemistry, Geophysics, Geosystems*, *19*, 1484–1498. https://doi.org/10.1029/2017GC007303

Túri, M., Palcsu, L., Papp, L., Horváth, A., Futó, I., Molnár, M., et al. (2016). Isotope characterization of the water and sediment in volcanic lake Saint Ana, East-Carpathians, Romania. *Carpathian Journal of Earth and Environmental Sciences*, *11*(2), 475–484.

van Soest, M., Hilton, D., & Kreulen, R. (1998). Tracing crustal and slab contributions to arc magmatism in the Lesser Antilles island arc using helium and carbon relationships in geothermal fluids. *Geochimica et Cosmochimica Acta*, *62*(19-20), 3323–3335. https://doi.org/10.1016/S0016-7037(98)00241-5

van Soest, M. C., Hilton, D. R., Macpherson, C. G., & Mattey, D. P. (2002). Resolving sediment subduction and crustal contamination in the Lesser Antilles Island arc: A combined he–O–Sr isotope approach. *Journal of Petrology*, *43*(1), 143–170. https://doi.org/10.1093/petrology/43.1.143

Varekamp, J., Kreulen, R., Poorter, R., & Bergen, M. (1992). Carbon sources in arc volcanism, with implications for the carbon cycle. *Terra nova*, *4*(3), 363–373. https://doi.org/10.1111/j.1365-3121.1992.tb00825.x

Vaselli, O., Downes, H., Thirlwall, M. F., Dobosi, G., Coradossi, N., Seghedi, I., et al. (1995). Ultramafic xenoliths in Plio-Pleistocene alkali basalts from theEastern Transylvanian Basin: Depleted mantle enriched by vein metasomatism. *Journalof Petrology*, *36*(1), 23–53. https://doi.org/10.1093/petrology/36.1.23

Vaselli, O., Minissale, A., Tassi, F., Magro, G., Seghedi, I., Ioane, D., & Szakács, A. (2002). Ageochemical traverse across the Eastern Carpathians (Romania): Constraints on the origin andevolution of the mineral waters and gas discharge. *Chemical Geology*, *182*(2-4), 637–654. https://doi.org/10.1016/S0009-2541(01)00348-5

Vinkler, A. P., Sz, H., Ntaflos, T., & Szakács, A. (2007). Petrology and geochemistry of pumices from the Ciomadul volcano (Eastern Carpathians)—implications for petrogenetic processes. *Földtani Közlöny*, *137*(1), 103–128. In Hungarian

Wei, F., Xu, J., Shangguan, Z., Pan, S., Yu, H., Wei, W., et al. (2016). Helium and carbon isotopes in the hot spring of Changbaishan Volcano, northeastern China: A material connection between Changbaishan Volcano and the west Pacific plate. *Journal of Volcanology and Geothermal Research*, *327*, 398–406. https://doi.org/10.1016/j.jvolgeores.2016.09.005

Wenzel, F., Lorenz, F. P., Sperner, B., & Oncescu, M. C. (1999). Seismotectonics of the Romanian Vrancea Area. In F. Wenzel, D. Lungu, & O. Novak (Eds.), *Vrancea earthquakes: Tectonics, hazard and risk mitigation*, (pp. 15–25). Netherlands: Springer.

Werner, C., Evans, W. C., Poland, M., Tucker, D., & Doukas, M. (2009). Long-term changes in quiescent degassing at Mount Baker Volcano, Washington, USA: Evidence for a staller intrusion in 1975 and connection to a deep magma source. *Journal of Volcanology and Geothermal Research*, *186*(3-4), 379–386. https://doi.org/10.1016/j.jvolgeores.2009.07.006

Wortel, M. J. R., & Spakman, W. (2000). Subduction and slab detachment in the Mediterranean-Carpathian Region. *Science*, *290*(5498), 1910–1917. https://doi.org/10.1126/science.290.5498.1910